Generation of a CRISPR/Cas based genome editing system for *mefv* gene in Familial Mediterranean Fever-specific induced pluripotent stem cells

by

Gülnihal Kavaklıoğlu

A Thesis Submitted to the
Graduate School of Science and Engineering
in Partial Fulfillment of the Requirements for
the Degree of

Master of Science
in
Molecular Biology and Genetics

Koç University

January 2016

Koç University

Graduate School of Sciences and Engineering

This is to certify that I have examined this copy of a master's thesis by

Gülnihal Kavaklıoğlu

and have found that it is complete and satisfactory in all respects,
and that any and all revisions required by the final
examining committee have been made.

Committee Members:

Tamer T. Onder, Ph. D. (Advisor)

Nesrin Özören, Ph. D.

Nathan Lack, Ph.D.

Date :

Abstract

The ability to derive induced pluripotent stem cells (iPSCs) from any individual has opened up the possibility to generate patient- and disease-specific cell culture models. Such models facilitate research into disease mechanisms and provide a platform for *in vitro* drug screens. A drawback of disease-specific iPSC models is the lack of genetically matched controls. Recent implementation of bacterial adaptive immune system known as clustered regularly interspaced short palindromic repeats (CRISPR) and CRISPR-associated (Cas) systems in mammalian cells as a new genome editing tool has provided unparalleled simplicity and precision to introduce site-specific changes into host DNA. A central aim of this thesis was to generate tools to implement a Crispr/Cas9 based system in an iPSC model of genetic inflammatory disease with a goal to replace disease-causing allele with its wild type counterpart.

Familial Mediterranean Fever (FMF) is a autosomal recessive autoinflammatory disease caused by the mutations in the *mefv* gene. FMF has a high carrier rate in Turkey and the most severe form of the disease result from homozygous M694V mutations. iPSCs were derived from one such FMF patient and the presence of the disease-associated mutations was confirmed by DNA sequencing. To target the disease allele, single chimeric guide RNAs targeting *mefv* sequence at the vicinity of the M694V mutation were designed and cloned into expression vectors. The functionality of Crispr/Cas9 components in mammalian cells were confirmed using a Green fluorescent protein (GFP) reporter assay in 293T cells. To monitor homologous recombination (HR), a reporter construct in which GFP sequence was interrupted by the targeted *mefv* sequences was generated. Different HR donor templates were tested and linearized plasmids were observed to be the most efficient. Next, the ability of the selected guide RNAs to cleave the endogenous *mefv* locus was confirmed by a mismatch-specific DNA endonuclease assay. However, we failed to detect a corrected allele upon introduction of the Crispr components and a repair template bearing the wild type *mefv* exon 10 sequences into patient-specific iPSCs. To facilitate detection of corrected allele, a new donor template bearing silent mutations that create new restriction sites was designed. This donor template will enable the use of restriction fragment length polymorphism assay (RFLP) for screening rare iPSC clones that are successfully corrected.

Özet

Herhangi bir bireyden uyarılmış pluripotent kök hücre türetilebilmesi, hastaya ve hastalığa özgü hücre kültürü modellemelerinin oluşmasına olanak sağlamıştır. Bu tür modeller hastalık mekanizmalarına yönelik araştırmayı hızlandırmış, yapay koşullarda ilaç taramalarının yapılabilmesi için platform sağlamıştır. Hastalığa özgü uyarılmış pluripotent kök hücre modellemelerinin güçlüklerinden biri genetik olarak eşit kontrollerin yokluğudur. Yakın zamanda bakteriye ait edinilmiş bağışıklık sisteminin (clustered regularly interspaced short palindromic repeats (CRISPR) and CRISPR-associated (Cas) systems) memeli hücrelerine uygulabilir kılınması yeni bir genom yazılımını türetmiş olup konak DNA'ya sekansa özgü değişimler oluşturabilmesi için basitlik ve kesinlik sağlamıştır. Bu tezde ana amaç Crispr/Cas9'a dayalı bir sistemin ateşli genetik bir hastalığın uyarılmış pluripotent kök hücre modelinde uygulanabilmesi için araçlar oluşturmak ve hastalığa neden olan aleli yabanıl tip kopyasıyla değiştirmektir.

Ailesel Akdeniz Ateşi *mefv* genindeki mutasyonlar sonucu ortaya çıkan otozomal çekinik otoinflamatuvar bir hastalıktır. Ailesel Akdeniz Ateşi Türkiye'de yüksek bir taşıyıcı oranına sahiptir ve hastalığın en ciddi biçimi M694V homozigot mutasyonlarda görülür. Bu durumdaki bir hastadan türetilen uyarılmış pluripotent kök hücreler ve hastalığa neden olan mutasyonlar DNA dizilemesiyle gösterilmiştir. Mutasyonlu aleli hedeflemek için mefv sekansını hedefleyen M694V mutasyonu yakınında bulunan tek ve kimerik rehber RNA'ler tasarlanmıştır ve anlatım vektörlerinin içine kopyalanmıştır. Crispr/Cas9 parçalarının memeli hücrelerdeki işlevselliği yeşil floresan haberci proteini (GFP) analiziyle insan embryonal böbrek hücrelerinde doğrulanmıştır. Homolog rekombinasyonu gözlemleyebilmek için yeşil floresan haberci protein sekansı, hedeflenmiş mefv sekansı tarafından sekteye uğratılmış bir haberci vektör kullanılmıştır. Değişik homolog rekombinasyon donör vektörleri test edilmiş ve en verimli olarak linearize vekörler seçilmiştir. Daha sonra, seçilmiş rehber RNA'lerin endojen *mefv* lokusunu kesebilme kapasitesi DNA bazlarındaki uyumsuzluğa yönelik DNA endonükleaz analiziyle gösterilmiştir. Ancak Crispr parçalarının ve *mefv* geni 10. exon sekanslarını içeren onarım vektörünün hastaya özgü uyarılmış pluripotent kök hücrelerine verilmesinden sonra düzeltilmiş alel saptanamamıştır. Düzeltilmiş alelin saptanmasını kolaylaştırmak için, belirsiz mutasyonlar ve yeni restriksiyon bölgeleri taşıyan farklı bir onarım vektörü tasarlanmıştır. Tasarlanan bu donör vektör ile restriksiyon fragment length polimorfizm analizi (RFLP) yapılıp başarılı olarak düzeltilen seyrek olarak bulunan uyarılmış pluripotent kök hücre klonlarının taranması sağlanacaktır.

Acknowledgements

First and foremost, I would like to express my deepest gratitude to my advisor Dr. Tamer Önder who has always been supporting, encouraging and patient. I will always remember his calmness and soothing approach whenever I feel frustrated of going back to the drawing board. I will always be grateful to him for his support when I least deserved but needed the most and teaching me how to think wisely.

I would like to thank Dr. Tuğba Bağcı-Önder for reminding me I have a right to be who I am and how I am.

I would like to thank Dr. Nathan Lack and Dr. Nesrin Özören for giving their time and efforts to be in my thesis committee and precious feedback for improving my work.

I would like to acknowledge the financial support of the Scientific and Technological Research Council of Turkey (TÜBİTAK) and Koç University during the course my graduate study.

My sincere thanks go to the members of Önder Lab; Ayyub Ebrahimi for dealing with my never-ending questions without hesitating, Burcu Özçimen for amazing me with her tidiness, Can Aztekin for his straightforwardness and terrible movie suggestions, Deniz Uğurlu for always being ready to listening to me, Duygu Payzın for showing me fine details of protocols, Eda Süer for sharing her useful experiences and witty humor and Kerem Fidan for his funny notes he left on my desk almost every week. I would also like to thank ex-member of Önder Lab, Mehmet Uğur Girgin for being a great benchmate and making the lab work funnier. I owe special thanks to my precious friends and colleagues Ezgi Kaya, Fatma Özgün, Filiz Şenbabaoğlu, İbrahim Çağrı Kurt, Ahmet Cingöz, Uğur Gatfar, Fidan Şeker, Gülben Gürhan and Hilal Saraç for their invaluable friendship.

Special thanks to my best friends Merve Şen, Fatma Damak and Vedat Engin for our fun memories and Korhan Türker for his motivation although we are far from each other.

I would like to thank the best flatmates I ever had, Lauren Davis for her delicious cakes and Ferda Canbaz who literally made this thesis possible with her technical knowledge and introducing Kömür into my life. You will be deeply missed. Also I would like to thank Berkay Yıldırım for his continuous support, love and patience.

Finally, I thank to my parents, Fethiye and Mustafa for their never-ending love and raising me as a free spirit, and my sister Bahar for reading me The Children of Captain Grant aloud when we were kids. I hope to make you proud in the end.

So long and thanks for all the fish.

Table of Contents

Abstract iii
Özet iv
Acknowledgements v
Table of Contents vii
List of Figures ix
List of Tables x
Nomenclature xi
CHAPTER 1 1
INTRODUCTION 1
1.1. Induced Pluripotent Stem Cells 1
1.1.1. General mechanisms of reprogramming 2
1.1.2. Disease modeling with human induced pluripotent stem cells 5
1.1.3. Challenges in disease modeling 7
1.2. Genome Engineering Strategies 8
1.2.1. Zinc Finger Nucleases (ZFNs) 10
1.2.2. Transcription Activator-Like Effector Nucleases (TALENs) 11
1.2.3. Crispr/Cas9 13
1.2.3.1. Development and Mechanism of Crispr/Cas9 systems 13
1.2.3.2. Components of Type II CRISPR system 14
1.2.3.3. Application Crispr/Cas9 system in human induced pluripotent stem cells 16
1.3. Familial Mediterranean Fever 19
CHAPTER 2 22
MATERIALS AND METHODS 22
2.1. Maintenance and expansion of human iPSCs 22
2.2. Design and cloning of sgRNAs and *mefv* repair template 22
2.3. Generation of 293T cells stably expressing GFP 24
2.4. Generation of EGFP-deficient 293T cells 25
2.5. Generation of pegip-mefv-100bp construct 25
2.6. Transfection of 293T cells and FMF patient iPSCs 26
2.7. Surveyor Nuclease Assay 27
2.8. Amplification-Refractory Mutation System 28
2.9. Single cell isolation of 293T and THP-1 cells 28

2.10. Flow Cytometry ... 29
CHAPTER 3 ... 31
RESULTS ... 31
3.1. Validation of M694V mutation in both fibroblasts and iPSCs by sequencing 31
3.2. Characterization of iPSCs derived from FMF patients ... 32
3.3. Generation of a reporter system to assay Crispr/Cas9 components for DSB 33
3.4. GFP reporter assay confirmed homologous recombination in 293T cells 35
3.5. A reporter system validated the functionality of *mefv*-targeting sgRNAs in 293T cells 36
3.6. Linear donor template resulted in highest HR efficiency ... 37
3.7. *MEFV*-targeting sgRNAs generated DSB at endogenous *mefv* locus ... 39
3.8. Nucleofection of PBMC-iPSCs ... 40
3.9. Cleavage of mefv locus in patient-iPSCs ... 42
3.10. Detection of HR in FMF patient-derived iPSCs ... 43
3.11. Design of *mefv* donor template ... 44
CHAPTER 4 ... 45
DISCUSSION ... 45
4.1. Increasing the efficiency of homologous recombination ... 45
4.2. The specificity and off-target effects of Crispr/Cas9 ... 46
4.3. Increasing transfection efficiency of iPSCs ... 47
4.4. Investigating the role of pyrin in FMF in knockout cell lines ... 48
APPENDIX ... 49
BIBLIOGRAPHY ... 50

List of Figures

Figure 1. Representation of Crispr/Cas Systems in bacterial cells upon viral entry 14

Figure 2. Schematic representation of Cas9-gRNA targeting 16

Figure 3. The distribution of MEFV mutations and the domains of pyrin protein 20

Figure 4. Design of ARMS PCR primers for wild type and mutant MEFV alleles. 28

Figure 5. The validation of M694V mutation in both fibroblasts and iPSCs by sequencing... 31

Figure 6. Characterization of iPSCs derived from FMF patients and parent iPSCs. 33

Figure 7. Generation of a reporter system to assay to Crispr/Cas9 components for DSB. 34

Figure 8. GFP reporter assay to monitor homologous recombination. 35

Figure 9. Generation of a reporter system to test the functionality of sgRNAs targeting *mefv* sequence. 36

Figure 10. Testing different donor templates for HR efficiency. 38

Figure 11. Confirmation of double-stranded cleavage by *MEFV*-targeting sgRNA2 at the endogenous *mefv* locus. 40

Figure 12. Nucleofection of iPSC with different conditions. 41

Figure 13. Double-stranded cleavage by G2 in patient iPSCs. 42

Figure 14. Diagram for the detection of HR in patient iPSCs. 43

Figure 15. Design of a new *mefv* donor template. 44

Figure A.1. Design and verification of gRNAs for *MEFV* knock-out cell lines. 49

List of Tables

Table 1. Gene correction in iPSCs by genome editing tools 9

Table 2. *mefv* exon10 targeting gRNAs 23

Table 3. List of primers for *mefv* exon 10 amplification, repair template design and T7 endonuclease assay 24

Table 4. List of vectors and their corresponding figures 30

Nomenclature

AP	Antartic Phophatase
ARMS	Amplification-Refractory mutation system
Cas	CRISPR-associated system
CRISPR	Clustered regularly interspaced palindromic repeats
crRNA	Crispr RNA
DAMP	Danger-associated molecular pattern
DMEM	Dulbecco's Modified Eagle's Medium
DNA	Deoxyribonucleic acid
DSB	Double-stranded break
E8	Essential 8
EDTA	Ethylenediaminetetraacetic Acid
ESC	Embryonic stem cells
EtOH	Ethanol
FBS	Fetal bovine serum
FGF	Fibroblast Growth Factor
FMF	Familial Mediterranean Fever
GFP	Green fluorescent protein
gRNA	Guide RNA
HDR	Homology-directed repair
hiPSC	human induced pluripotent stem cells
IL-1β	Interleukin 1 Beta
iPSC	Induced pluripotent stem cells
MEF	Mouse embryonic fibroblast
MEFV	MEditerranean FeVer
MOI	Multiplicity of infection
mRNA	Messenger RNA
NHEJ	Non homologous end joining
OSKM	Oct4 Sox2 Klf4 Myc
PAM	Protospacer adjacent motif
PAMP	Pathogen-associated molecular pattern
PBS	Phosphate buffered saline

PEG	Polyethylene glycol
PNK	Polynucleotide kinase
PYD	Pyrin Binding domain
reTALEN	Re-coded TALEN
RFLP	Restriction fragment length polymorphism
RNA	Ribonucleic acid
ROCK	Rho kinase
rpm	Revolutions per minute
RT	Room temperature
sgRNA	Single guide RNA
SpCas9	*Streptococcus pyogenes* Cas9
SSEA	Stage-specific embryonic antigen
ssODN	Single stranded oligonucleotide
TALEN	Transcription activator like effector nuclease
tGFP	Truncated green fluorescent protein
tracrRNA	Trans-activating Crispr RNA
ZFN	Zinc Finger nuclease

CHAPTER 1

INTRODUCTION

1.1. Induced Pluripotent Stem Cells

The major source of pluripotent stem cells have traditionally been embryonic stem cells (ESC) which are derived from inner cell mass of blastocysts. These cells have the capacity to proliferate continuously while maintaining pluripotency, as they retain the ability to differentiate into various kinds of cell types. While a promising source of cell for clinical cell replacement therapies, their use has been problematic because of ethical concerns. In 2006, Takahashi and Yamanaka identified the factors that induce pluripotency in somatic cells [1]. Starting with 24 candidate genes, they further narrowed the candidates down to four by using a reporter gene driven G418 resistance as a detection mean for pluripotency. The resulting four factors that can reprogram somatic cells into induced pluripotent stem cells (iPSCs) were identified as Oct3/4, Sox2, Klf4 and c-Myc[1]. The reprogrammed cells express ESC markers such as Oct3/4, Sox2, Nanog, exhibit demethylation of Oct3/4 and Nanog promoters, are positive for alkaline phosphatase and SSEA-1, and can form teratomas in nude mice, all of which demonstrate their pluripotency. In addition, mouse iPSCs derived from GFP-expressing mouse tail-tip fibroblasts under CAG promoter were able to generate embryos containing GFP-positive iPSCs when they are microinjected into blastocysts proving their ability to contribute to chimeras [1]

A following study by Takashi and Yamanaka demonstrated that human dermal fibroblasts can also be reprogrammed into human induced pluripotent stem cells (hiPSCs) by retroviral introduction of the same set of four factors [2]. hiPSCs expressed ES cell-like markers Oct3/4, Sox2, Nanog, Gdf3, Fgf4 as well as becoming positive for SSEA-3, SSEA-4, tumor-related antigen 1 (TRA-1-60), TRA-1-81 and alkaline phosphatase. hiPSCs displayed exponential growth, high telomerase activity, and the ability to differentiate into three germ layers in embryoid bodies and teratomas [2]. Alternatively, Thomson and colleagues observed that human somatic cells can be reprogrammed into iPSCs by the introduction of Oct3/4, Sox2, Nanog and Lin28[3]. The expression of ES cell-like markers, teratoma formation, increased telomerase activity and karyotype analysis all proved that hiPSCs generated via these four factors are functionally indistinguishable from ES cells[3].

Pluripotency in both mouse and human somatic cells is established through the expression of *Oct3/4* and *Sox2*[4]. However, downstream regulations differ such that there seen variations epigenome, transcriptome, self-renewal and differentiation capacities, which may temper the generation of human iPSCs compared to that of mouse iPSCs. In addition, c-Myc has a negative role in the self-renewal of human embryonic stem cells provided that ectopic expression of c-Myc leads to differentiation and apoptosis of ES cells. In contrast to human ES cells, mouse ES cells are positively affected by the exogenous expression of c-Myc[2].

1.1.1. General mechanisms of reprogramming

There are distinctive stages in the process of reprogramming somatic cells to generate iPSCs[5]. The first stage begins with the induction of proliferation and the downregulation of fibroblast-specific genes. Before the upregulation of pluripotency-related genes, cells gain epithelial characteristics by expressing genes such as E-cadherin and stage-specific antigen 1 (SSEA-1). At the late stage, pluripotency-related gene promoters are demethylated resulting in a more open chromatin structure which is followed by the binding of reprogramming factors to establish pluripotency [5].

Reprogramming is a highly inefficient process. The inefficiency is due to several factors one of which is the variability in the stoichiometry of four the exogenously expressed factors. Even though a large proportion of the initial cells express all the reprogramming factors, they do not necessarily end up as iPSC colonies at the end of the process. It is known that the differentiation status of the starting cell populations have an effect on the efficiency of reprogramming. Hematopoietic stem or progenitor cells produce iPSC colonies 300-fold higher than terminally differentiated cells do[6]. One study also showed that all target pre-B-cell populations can give rise to iPSCs when they were cultured for longer periods[5]. In addition, insertional mutagenesis caused by lentiviral vectors was thought to reduce the reprogramming efficiency. The data coming from the use of non-integrative reprogramming vectors and secondary reprogramming technique in which defined integration site is present in the all cells of the mice eliminated the possibility. The first one involving oriP/EBNA1 plasmid yielded 3 to 6 colonies per million transfected cells[7]. The latter, on the other hand, had reprogramming efficiency ranging from 0.26% to 2% [8]. The choice of donor cell type affects the efficiency and the quality of iPSCs. Most of the iPSCs use fibroblasts as donor cells. However, human primary keratinocytes was shown to be reprogrammed more efficiently than fibroblasts[9]. Cord blood $CD133^+$ cell can be reprogrammed with only *Sox2* and *Oct4* transduction. Based on the examples, the choice of the donor cell type determines the kinetics of reprogramming process[10].

In the generation of iPSCs, the combination of reprogramming factors influences the donor cells in terms of pluripotency, cell proliferation and epigenetics. Several combinations of the four factor (OSKM) together with chemical compounds that alter chromatin modifications, miRNAs and enzymes are all examined for their effect on reprogramming [10]. For example, *Nanog* expression with OSKM in mouse B cells accelerates the appearance of iPSC colonies[11]. *Utf1*, a pluripotency transcription factor, has been shown to increase the number of AP^+ cells in human dermal fibroblasts[12]. Similarly, *Sall4* has found to elevate iPSC generation when transduced with OSK[13]. Human telomerase reverse transcriptase (hTERT) and SV40 large T antigen (SV40LT) promote cell proliferation in combination with OSKM[14]. In addition, a chemical compound that acts as a mitogen-activated kinase kinase (MEK) inhibitor has been shown to increase the number of iPSCs in combination with *Klf4* and *Oct4*[15]. Expression of miR-290 cluster increased the number of GFP^+ iPSC colonies when they are introduced to *Oct4-GFP* MEFs[16]. Chromatin remodeling complexes have also an effect on reprogramming as evidence by the increased efficieny in reprogramming upon treatment with certain histone deacetylase (HDAC) inhibitors such as suberoylanilide hydrotaxamide acid (SAHA), trichostatin A (TSA), butyrate and valporic acid (VPA) enhance reprogramming [17].

There are two major ways in which the four Yamanaka factors can be delivered into somatic cells. These can be classified as integrating and non-integrating delivery methods.

One of the initial integrating methods to introduce reprogramming factors into donor cells has been retroviral delivery[10]. Some of Moloney monkey leukemia virus (MMLV)-derived retroviruses used in this methodology are pMXs, PLib and PMSVCs. Their cloning capacity is 8kb. They infect dividing cells and the retroviral genes are silenced through reprogramming, which is desired for the quality of iPSCs. The reprogramming efficiency, however, is 0.1% in MEFs, 0.01% in human fibroblasts. The other major viral delivery system is HIV-derived lentiviral vectors. These generally can be produced at high titer and their cloning capacity is higher than MMLVs-derived retroviruses, ranging between 8-10kb. They are able to infect both dividing and non-dividing cells. The efficiency of reprogramming with these vectors is comparable to MMLV-derived retroviruses. A disadvantage of the lentiviral vectors is that transgene silencing is less robust but this can be overcome with the use of tet-inducible systems [10]. In general viral delivery of the four factors has some drawbacks, one of which is that the random integration of the viruses might disrupt tumor-suppressor genes if they are integrated in ORFs. They also cause the formation of heterogeneous iPSC colonies, which hampers comparative analysis. Reactivation of silenced transgenes can occur during differentiation or transplantation due to tissue-specific activation, causing tumor formation. This, however, has been overcome by Cre-deletable and inducible lentiviruses[10].

The second way to introduce OSKM into the donor cells is transfection of linear DNA via liposomal transfection or electroporation. The use of polycistronic vectors with self-cleaving (2A) sequences showed that single copy of the vector is sufficient to produce iPSCs colonies. 10% of the iPSC colonies have been shown to have a single copy of such transfected transgenes. However, the efficiency of transfection is too low in this approach. Combined with the low efficiency of reprogramming, this system requires too many donor cells to obtain one single iPSC colony generation. Another disadvantage is that when this vector is flanked by *loxP* sites and deleted by transient *Cre* recombinase expression, iPSC colonies start to differentiate meaning that their self-renewal is not maintained[10].

The third method is the use of PiggyBac transposon (PB). PB facilitates the integration of the transgenes. The vector includes the transposon and is co-transfected with a helper plasmid containing the transposase. The advantage of PB is that it leaves no genomic scar as *Cre* or FLT recombinase do [18]. Therefore, it enables precise deletion of transgenes. The drawback of PB is that it has an increased rate of non-conservative deletion events due to transposase activity [10].

Non-integrative delivery system comprises of 4 methods: Transduction with integration-deficient viral vectors, episomal DNA, RNA and protein transfections. In most of these cases, both transfection and reprogramming efficiency is low and the generation of iPSC colonies takes several weeks. One of the earliest integration-deficient viral delivery utilizes adenoviruses, PHIHG-Ad2[19]. In one study, integration-free iPS cells have been obtained from mouse hepatocytes[19]. Another study showed the generation of diploid transgene-free iPSCs from human fetal fibroblasts[20]. Adenoviruses infect both dividing and non-dividing cells but the infection efficiency is very low, ranging between 0.0001% and 0.0018% in mouse[20].

Sendai-viral vectors are also non-integrative and are able to transfer foreign DNA into the host cell. They replicate constitutively as negative-sense ssRNA in the cytoplasm of the host cell. Therefore, it is difficult to eliminate them from the infected cells. Sendai viral vectors which express OSKM have been shown to reprogram human fibroblasts and T cells[21][22].

Transient episomal delivery is simpler than viral delivery. MEFs can give rise to iPSCs either with a serial transfection of two plasmids, OSK and *myc* or with a polycistronic vector expressing OSKM. Out of iPSCs colonies, only 33% and 8% was integration-free. Yet, human fetal fibroblasts and keratinocytes have failed to produce iPSCs. The problem might result from the low transfection efficiency of large plasmids, inappropriate dilution of the vectors and the silencing of prokaryotic sequences present at the vector backbone [23],[24]. The use of oriP/EBNA1 vector which are maintained during the cell divisions eliminated the serial transfections and dilutions of the episomal vectors. *Yu et al*, 2009 succeeded in generating iPSCs from HFFs with the aid of oriP/EBNA1 together with OSK and Nanog, OSK and SV40LT,*Myc* and *Lin28*, respectively[25]. The same procedure, when applied to human fibroblasts, yielded only 3 to 6 iPSC colonies per million transfected cells, which was extremely low.

The third option for non-integrative delivery is through RNA. Direct delivery of synthetic mRNAs into donor cells has been established [26]. The study proved that the reprogramming efficiency is higher than that of other non-integrative systems. 2% of neonatal fibroblasts gave rise to iPSC colonies in 17 days. In this system, mRNAs are modified to be protected from endogenous antiviral cell defense response. RNA delivery is simple and efficient yet labor intensive and expensive to implement.

Finally, protein delivery method can be utilized to exclude unnecessary genetic material in the donor cells. For that, proteins are co-delivered with HIV transactivator of transcription (Tat) or polyarginine. In one study, Oct4-GFP MEFs were serial transduced with poly-arginine-tagged recombinant OSKM proteins. When HDAC inhibitor, VPA was supplied, iPSC colonies emerged[27]. However, protein delivery is highly inefficient and labour-intensive.

1.1.2. Disease modeling with human induced pluripotent stem cells

The basic instruments to study disease mechanisms have traditionally been animal models and human cell culture. However, there are limitations in animal models of human diseases. Firstly, mouse models do not completely recapitulate human diseases due to differences in their genomes. Likewise, many genetic variants related to human diseases are located in non-coding regions. Since these regions are not conserved in mice, their potential contributions to the disease phenotypes cannot be observed. The other reason for the lack of representation of human diseases in animal model is that some disease mutations in animals are lethal. Moreover, the drugs used in animal models may not necessarily be as effective in humans, hindering drug screens.

The ability to generate pluripotent cells in a personalized manner has been very useful in understanding of disease mechanisms and has the potential to revolutionize regenerative medicine. Owing to the availability of somatic cells from individuals with the disease via skin biopsy or cord blood, disease- and patient-specific iPSCs could be derived and then differentiated into diseased cell type on demand. One of the advantages of the technology is to provide the affected cell type which is normally difficult to derive from patients and culture them indefinitely.

The beginning of iPSC-based disease modeling was with the generation of iPSCs derived from aged ALS patients[28]. In this study, iPSCs were differentiated into motor neurons, which are the diseased cells in ALS. Another study generated iPSCs from adenosine deaminase deficiency-related severe combined immunodeficiency (ADA-SCID), Scwachman-Bodian-Diamond syndrome, Gaucher Disease type III, Duchenne and Becker muscular dystrophy, Parkinson disease, Huntington disease , juvenile-onset, type 1 diabetes mellitus, Down syndrome and the carrier state of Lesch-Nyhan syndrome patients[29]. Patient-derived iPSCs were differentiated into embryoid bodies to confirm their pluripotency. Teratoma formation assays in immunosuppressed mice were successful producing three germ layers. This study enabled a platform to compare normal and diseased cells to understand pathology of the disease. Disease modeling with the aid of iPSC technology facilitates the study of monogenic diseases as well as complex ones. Some examples include : Hematological diseases such as β-thalassemia, Fanconi anemia, neurological diseases such as Spinal muscular atrophy, Frontotemporal dementia and metabolic diseases such as Wilson's disease, Type I diabetes etc (see also Table 1) [30].

There is an increasing number of studies in literature exemplifying disease pathology in patient-derived iPSCs. For example, one such study focused on Chronic infantile neurologic cutaneous and articular syndrome (CINCA) caused by mutations the *NLRP3* gene[31]. The mutations exhibit somatic mosaicism hampering the description of CINCA pathogenesis. By generating NLRP3-mutant and nonmutant iPSCs and differentiating them into macrophages which are the affected cell type in CINCA, mutant iPSC-derived macrophages were distinctively found to secrete IL-1β at abnormal levels. The authors demonstrated that disease-related phenotype was caused by *NLRP3* mutation. Large quantity of NLRP3-mutant iPSCs was also instrumental for a drug screen. This study employed anti-inflammatory compounds available for drug screen and revealed that increased IL-1β secretion could be prevented by certain drug compounds.

The second utility of the patient-derived iPSCs is the ease of drug screens on the affected cell lines. Testing candidate small molecules on diseased-cell types derived from patient-specific iPSCs is dependant on the abilty to detect disase-specific phenotypes. Disease-related phenotypes are either mitigated or sustained upon the application of candidate small compounds. This technique has been very informative in a model for spinal muscular atrophy (SMA) and Rett syndrome [32],[33]. For instance, valproic and tobramycin has been found to be effective in SMA-specific cells elevating neural survival[32]. IGF1 treatment has increased glutamatergic synapse number and resulted in changes in neural morphology in neurons differentiated from Rett-iPSCs [33]. In another example, the antipsychotic Loxapine has increased neuronal connectivity and the expression of several glutamate receptor in Schizophrenia-iPSCs [34].

1.1.3. Challenges in disease modeling

A crucial factor in disease modeling is to observe a disease-related phenotype in iPSCs to compare with that of controls. However not all patient-derived iPSC display an overt cell-culture phenotype. This is more likely to be the case when modeling sporadic or late-onset diseases. For example, iPSCs derived from sporadic Parkinson's disease patients do not show distinctive phenotype when differentiated and compared to controls [35]. Other examples include type I diabetes, Down syndrome and Crigler-Najjar syndrome [36].

Variability among patient-derived iPSC clones is another constraint in disease modeling with iPSC. The heterogeneity of iPSCs might stem from the methods by which iPSCs are produced, the subsequent culture media, the factors to which they have been exposed and the viral integration site and number[37]. Additionally, it is affected by the age, gender and the ethnicity of donor individuals. The other reason for variability of iPSCs is the epigenetic state of starting somatic cells. It is known that iPSCs retain epigenetic traces of somatic cells from which they are originated[37]–[39].Some iPSCs lose this residual epigenetic memory as they are continually passaged in culture.

The main rationale in disease modeling is to compare the diseased and healthy phenotype distinguished by DNA variants, with an isogenic background. In other words, it is especially crucial to have rigorous controls which are genetically as similar as possible to the patient-derived iPSCs. The discrepancy between control and patient iPSCs stems primarily from differences in genetic background. In many studies the controls are generally derived from unrelated healthy individuals who have a different genome than the patients. However, ideally genetically matched controls would be wild type and mutant cells would differ only in the disease causing mutation[37].

Having an isogenic control is more reliable and has become plausible with gene editing technologies. To induce the disease-causing mutation in the parental cell line or to correct the mutation in the patient-derived cell line would be both beneficial depending on the disease type. In that case, working with multiple clones of the selected colonies has been advised due to potential mutations which might arise during clonal isolation[40][41].One example of such approach has been used in ALS modeling in which a non-cell autonomous effect on the motor cells was observed [42]. Yet, the most important question during comparison of controls and patient-derived iPSC colonies is that if idiosyncratic differences between iPSCs or the disease-related DNA variants actually cause the disease-related phenotype in patient-iPSCs.

The improvements in reprogramming methods and gene-editing strategies have decreased the variability among iPSCs, thus mitigating one of the main drawbacks of the iPSC-based studies. Gene editing strategies have enabled the generation of isogenic parental cell lines whereas advancements in reprogramming methods expedite the generation of a large number of patient-derived iPSCs. Improvements in both of these technologies conditions will enable the generation of more reliable control groups leading to the discovery of disease-causing mutations and form a platform for screening small compounds.

1.2. Genome Engineering Strategies

Making site-specific changes on the genomes of various organisms has been envisioned since the discovery of the DNA double helix. Provided that cells have internal mechanisms to repair double-stranded breaks which otherwise would be fatal, the early approaches for site-specific recognition and cleavage started with the use of oligonucleotides and small molecules [43].

The first study utilized oligonucleotides along with bleomycin or psoralen which are cross-linking agents in mammalian and yeast cells [44], [45] Next, self-splicing introns were used[46], leading to design of artificial nucleases that can cleave DNA. One study produced such artificial endonuclease by combining the domains of homing nucleases[47]. With the generation of zinc-finger nucleases (ZFNs) and transcription activator-like effector nucleases (TALENs), genome editing became much more promising.

Table 1. Gene correction in iPSCs by genome editing tools

Disease	Gene(Mutation)	Technique	Reference
Cystic fibrosis	*CFTR*	CRISPR	[48]
		ZFN	[49]
Beta-thalassemia / Sickle cell disease	*HBB* (IVS2-654) C/T	CRISPR&TALEN	[50]
	HBB 69(A/T)	CRISPR	[51]
	HBB -28 (A/G) and 4-bp deletion	CRISPR	[18]
	HBB CD17 (A-T)	CRISPR	[52]
	HBB	ZFN	[53]
HIV	*CCR5*	ZFN	[54]
		CRISPR	[55]
Myeloproliferative neoplasm	*JAK2* (V617F)	CRISPR	[56]
Alpha1- antitrypsin deficiency	*ATT* (Z-ATT)		
Familial platelet disorder	*RUNX1* (Y260X)	ZFN	[57]
	R174X	TALEN	[58]
X-linked chronic granulomatous disease (X-CDG)	*NOX2*	TALEN	[59]
Chronic granulomatous disease (CDG)	*CYBA, NCFI,NCF2, NCF4*	ZFN	[60]
Duchenne Muscular Distrophy	*DMD*	CRISPR&TALEN	[61]
Frontotemporal dementia	*GRN*(IVS1+5G>C)	ZFN	[62]
Cardiomyopathy	*PLN* (R14*del*)	TALEN	[63]
Severe combined immunodeficiency	*PRKDC*(Y4046*)	ZFN	[64]
Fanconi anemia	*FANCA*	HR dependent gene editing	[65]
Alpha-1 antitrypsin deficiency	*ATT* (Q342K)	TALEN	[66]
Hemophilia A	*F8*	TALEN	[67]
Parkinson’s Disease	*LKRR2*	ZFN	[68]
Tauopathy	*TAU* (A152T)	ZFN	[69]
Huntington Disease	*HTT*	HR-dependent gene editing	[70]

1.2.1. Zinc Finger Nucleases (ZFNs)

One of the tools of targeted genome engineering is zinc finger nucleases which cause cleavage in the genome followed by a repair mechanism. It leads to several gene modifications in the genome. These modifications include gene knockout, gene addition and homology-based repair. The examples of such modifications have been shown in model organisms such as *Drosophila melanogaster*, zebrafish, rats, *Arabidopsis thaliana*, some crop species, as well as human embryonic stem, haematopoietic stem and induced pluripotent stem cells [71][69][70].

Zinc finger nucleases (ZFNs) combine site-specific DNA-binding domains and the endonuclease domain of bacterial FokI restriction enzyme[71]. Zinc-finger domains recognize 3 bp DNA sequence and they can be arranged in tandem to specifically target the DNA. Each zinc finger determines base-specific binding and binds to 3-bp target in the genome thanks to a region of tandem array of Cys2-His2[74]. Each ZFN contains three to six zinc fingers to target 9-24bp DNA. Modular assembly approach is used for making ZFNs and is based on functional autonomy of individual fingers on DNA. To eliminate potential off-target effects which might stem from unspecific complementarity, ZFNs must be designed to target recognition target sequences which are expected to be unique within the genome.

The second feature of a zinc finger nuclease is to include a zinc finger protein with a *FokI* nuclease domain. This domain plays a role in cleavage generation in the genome when there is complementarity between DNA binding site and the target sequence. The cleavage is strictly restricted to binding. FokI catalytic domain catalyzes double stranded breaks (DSBs) and the most important point is that it has to dimerize to function[75]. DSB is generated only when correct orientation and appropriate spacing between the dimers occurs. Upon binding, the FokI domains dimerize and catalyze DSBs with 5' overhang. Resulting DSB is repaired by nonhomologous end joining (NHEJ) or homology-directed repair (HDR). NHEJ is employed to induce frameshift mutations at the target gene whereas HDR is used for precise editing or correcting with a concomitant donor template. HDR is utilized only when there is a template strand such as a plasmid or single stranded oligonucleotides (ssODNs). NHEJ does not require the presence of a template strand.

ZFNs have been shown to carry out genome editing in various organisms with different efficiency. Gene disruption in *D.melanogaster* yielded 10% efficiency with ZFNs[76]. In zebrafish 50% of targeted clones showed germline mosaicism[77]. In rats, extended recognition sites and stable transgenesis of inducible ZFNs were used generating SCID mice[78]. First application of ZFNs in endogenous *Dhfr* locus in mammalian cells was with Chinese hamster ovary cells (CHO) resulting in 15% efficiency[79]. As for HDR-based studies, in mammal cells, *IL2RG* gene was targeted in K562 cells by creating *de novo* point mutations with 20% efficiency and 8% showed biallelic modification[80]. In ES cells, 6% targeting efficiency was obtained without selection and stable gene expression occurred[81]. In human mesenchymal stem cells, the efficiency was 50% without selection[82].

Several studies have focused on gene editing in iPSCs using ZFNs (Table 1). One such study dealt with sickle cell anemia, caused by E6V mutation in β-globin gene, in three different iPSC lines [53]. After characterization of SCD-iPSCs with ESC markers, karyotyping and teratoma formation assay, SCD-iPSCs were transfected with ZFNs along with introduction of a donor template containing wild type sequence for the β-globin gene. The confirmation of donor template integration and successive correction of the mutation provided a proof-of-principle study in ZFN-mediated gene editing.

1.2.2. Transcription Activator-Like Effector Nucleases (TALENs)

Transcription activator-like effectors (TALEs) are DNA-binding domains and when combined to FokI nuclease they constitute TALENs and enables site-specific targeting [83]. TALEs were discovered in the plant pathogen *Xanthomonas* where they drive the expression of effector-specific genes in the host plant cells [84]. These repeats were characterized as a novel DNA-binding domain. TALE repeats consist of tandem arrays with 10-30 repeats, each includes 33 to 35 amino acids[83]. Each repeat also contains two additional amino acids, the repeat-variable-diresidue (RVD), which specify the cognate nucleotide [85]. The emergence of TALENs was based on the idea of changing RVDs. By the alterations in RVDs, the target of TALE repeats could be determined, enabling target choice flexibility. Similar to ZFNs, TALE domain fused to *FokI* endonuclease domain lead to TALENs which are site-specific nucleases [86]. TALENs generate DSBs on the genome to be repaired by NHEJ or HDR.

TALENs proved to be efficient in genome editing in hiPSCs and hESCs[87]. The experiments on different hiPSC lines showed 2-34% indel rate by NHEJ depending on the cells and 1.6% HDR-based knockin rate. The same study also showed low off-target effects. As an example, Hemophilia A, a genetic blood disorder was studied with TALENs[67]. Mutations in blood coagulation factor VIII (*F8*) were targeted by TALEN pairs to invert 140 kbp chromosomal segment on the F8 gene as this type of chromosomal inversions is the most frequent observed.

Additionally, they inverted back the segment to obtain normal positioning. Similar to the study with ZFNs, after generating patient-specific iPSCs, they were confirmed for pluripotency. TALEN pairs were transfected into patient-derived iPSCs and checked for inversion by PCR to two inversion breakpoints. About 1.4% inversion efficiency was seen in hiPSCs. The same TALEN pair also reversed the inversion with 1.3% efficiency. Resulting corrected iPSCs showed F8 mRNA and protein expression as wild type cells proving that *F8* expression was restored with TALENs.

Compared to ZFNs, TALENs are relatively easier and time-efficient to design. Knowing that ZFNs are able to target 9-24 bp sequences in-length, TALE repeats can be engineered to target more extended DNA sequences. Although binding affinity was found as high as 96%, the extended targets may result in decrease in binding affinity to DNA [88]. One of the other advantages of TALEN is to cause less off-target effects and toxicity than ZFNs when they are introduced into cells[89]. TALENs were especially shown to have very low off-target effects on hiPSCs based on a whole-genome sequencing study[90], [91].

There are some limitations on TALEN-based studies. The first one is the large size of TALENs whose cDNA is around 3kb. This hampers the delivery of TALENs into the cells. Parallel to that, the use of viral delivery due to its large size makes it inappropriate for gene therapy. The second disadvantage of TALENs is the repetitive sequences which impair their lentiviral-based delivery because TALEN sequences are not stable such that rearrangement can occur following their lentiviral delivery[92]. However, re-coded TALENs (re-TALENs) were optimized by eliminating direct or inverted repeats longer than 11 bp in order to improve the delivery and the expression of TALENs[93].

The design and the synthesis of the proteins for both ZFNs and TALENs are difficult and time-consuming. Recent adaptation of Crispr/Cas9 system from bacteria as a gene-editing tool started a new era in genome engineering technology with its simplicity and cost-efficiency

1.2.3. Crispr/Cas9

1.2.3.1. Development and Mechanism of Crispr/Cas9 systems

Crispr/Cas is a bacterial and archaeal immune system in which RNA-guided nucleases cleave foreign DNA or RNA[94]–[96]. CRISPR loci in bacteria or archaea involve CRISPR-associated genes (Cas) and a CRISPR array. CRISPR array consists of repetitive sequences (direct repeats) distributed among short variable sequences, from which it takes its name: Clustered regularly interspaced palindromic repeats [97]. These short variable sequences stem from invading DNA called protospacers that get incorporated into bacterial genomes. Protospacers are called spacers in host DNA and they are flanked by protospacer adjacent motifs (PAMs). CRISPR arrays are first transcribed into a single RNA and processed into shorter CRISPR RNAs (crRNAs). These small RNAs base-pair with protospacers within foreign DNA and guide a multifunctional protein complex including Cas protein to recognize and cut the invading DNA [94].

The repetitive sequences (spacers) were first described in *Escherichia coli* and include 29 nt. repeats that were interspersed with 32 nt. nonrepetitive sequences [98]. Later, as new clusters of repeats were discovered in other microbial species, they were classified as clustered repeat elements [99]. One of the intriguing findings came about in 2005 suggesting the extrachromosomal origin of the spacers [100], [101]. Its been shown that viruses were unable infect the host cells with spacers matching with their genomes suggesting a role for spacers in immunity and defense.

There are three types of CRISPR system. Type II CRISPR system was discovered in *Streptococcus thermophiles* and its role in adaptive immune system was demonstrated[102]. Type I CRISPR found in *E. coli* was shown to transcribe CRISPR array and further process it into small Crispr RNAs (crRNAs) containing individual spacers[103]. Later, Type III CRISPR studied in *Staphylococcus epidermidis* was demonstrated to impede plasmid conjugation via Cas activity[104].

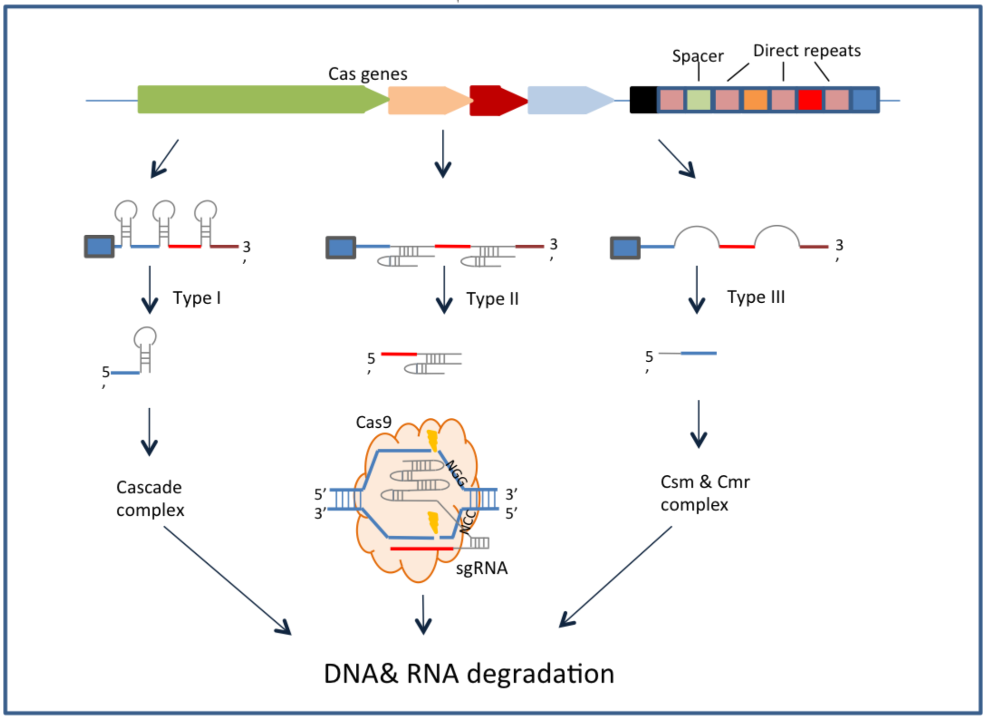

Figure 1. Representation of Crispr/Cas Systems in bacterial cells upon viral entry (Adapted from [105])

1.2.3.2. Components of Type II CRISPR system

Unlike type I and III, type II has substantially reduced number of Cas proteins and Cas9 is employed for cleavage. In addition type II system employs a noncoding trans-activating crRNA (tracrRNA) which hybridizes with crRNA to form a scaffold and facilitate the guidance of Cas9 (**Figure 2**). In adapting the type II system for use in mammalian systems crRNA and tracrRNA has been combined to generate a single chimeric guide RNA (gRNA) that can be efficiently transcribed as a single transcript. [106]

Cas9 consists of two nuclease domains: RuvC and HNH. The first one has a single nuclease domain while the latter has multiple subdomains. Single-particle electron microscopy revealed that the apo state (non-DNA binding state) of Cas9 is catalytically inactive and that it requires a structural activation for DNA recognition. Without DNA binding of gRNA, HNH domain is blocked by RuvC domain. Guide RNA enables the activation of Cas9 by triggering a conformational change within Cas9 [107]. Another structural study unraveled that the domain of SpCas9 in complex with sgRNA. It consists of an alpha-helical recognition site (REC),a nuclease lobe (NUC) with HNH and RuvC domains and a Protospacer adjacent motifs-interacting (PI) region [108]. These studies together show that Cas9 requires gRNA-

DNA hybridization in order to catalyze DSB. It also demonstrated that HNH nuclease domain of Cas9 cleaves complementary strands whereas RuvC nuclease domain cleaves noncomplementary strand.

Target recognition by gRNA/Cas9 complexes are achieved by Watson-Crick base pairing between the target sequence and protospacer of guide RNA (20-bp) at the 5' site. The hybridization also requires the presence of a Protospacer adjacent motif (PAM) at the 3' end of DNA target site (**Figure 2**) [109]. Single–molecule imaging showed that Cas9 bound to gRNA first interacts with PAM sequence preventing unbound Cas9 from unspecific interactions along the DNA [107]. PAM binding together with gRNA-DNA hybridization activates nuclease domains of Cas9 and trigger cleavage. PAM sequences are specific to Cas9 orthologs, meaning that its range depends on the Cas9 protein. For example, the PAM sequence of *Streptococcus pyogenes* Cas9 (SpCas9) is 5'-NGG[110]. It occurs in human genome at every 8 bp. SpCas9 can also bind to 5'-NAG but at a very lower rate. *S. thermophilus* has 5'-NNAGAAW as type I and 5'-NGGNG as type III. *Neisseria meningitidis* has 5'-NNNNGATT PAM sequence [111]. The variety of PAM sequences can be employed to targeting of different loci within the same cell. Alternatively, specificity of PAM can be altered, in which Cas9 from *S. thermophilus* could be used for 5'-NGG sequence by changing the PAM-interacting domain of Cas9 nuclease.

In 2012 purified Cas9 protein from *Streptococcus thermophilus* and *Streptococcus pyogenes* has been shown *in vitro* to target and cleave DNA, paving its way to gene editing [112]. In this study, both crRNA-tracrRNA hybrid and a single guide RNA (sgRNA) were used to cleave DNA. In 2013, four groups simultaneously showed that heterologous expression of Cas9 from *S. pyogenes and S.thermopilus* (codon optimized) when combined with a single chimeric gRNA (tracrRNA:crRNA) cause double stranded breaks (DSBs) at the target site in mammalian cells [109], [113], [114]. The cells used include human embryonic kidney, chronic myelogenous leukemia and induced pluripotent stem cells.

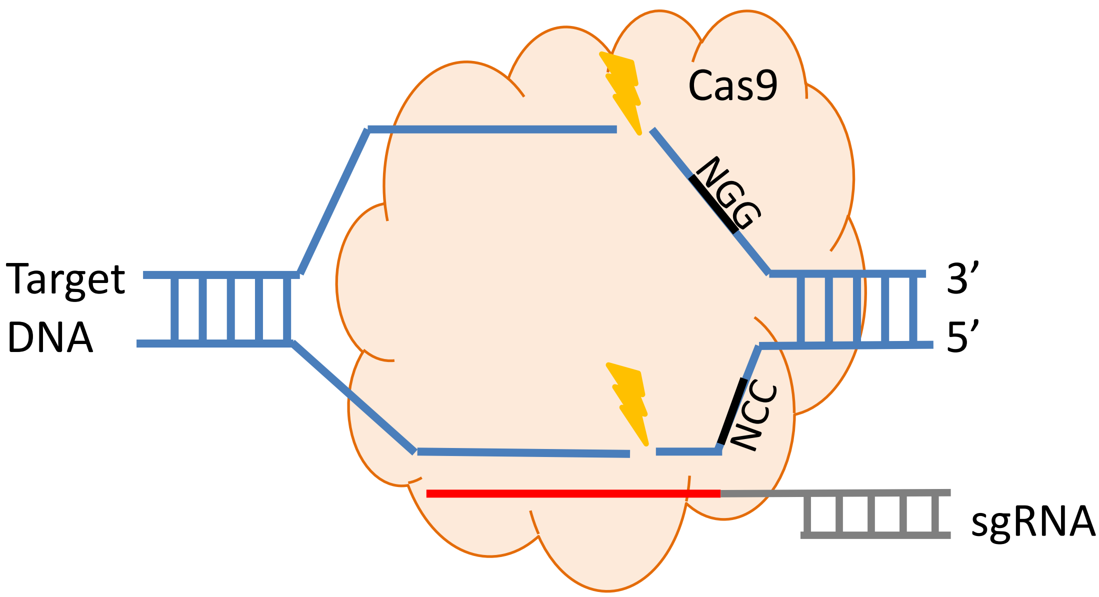

Figure 2. Schematic representation of Cas9-gRNA targeting

DSBs introduced on DNA lead to gene editing by nonhomologous end joining (NHEJ) and homology-directed repair (HDR). NHEJ is an error-prone intrinsic DNA repair mechanism in the cell, which can occur any time in case of a DSB. Homology-directed repair, on the other hands, occurs only when there is a repair template with homology arms. This period corresponds to late S and G_2 phase. The first mechanism may cause frame shifts on reading frame leading to truncated mRNAs [115] and truncated mRNAs are discarded by nonsense-mediated decay[116]. HDR is used for precise alterations on the genome such as gene correction or insertion. It requires a repair template in which desired genetic modification is present. Repair template could be single-stranded oligonucleotide (ssODN) or double-stranded DNA vector [117], [118].

1.2.3.3. Application Crispr/Cas9 system in human induced pluripotent stem cells

The implementation of Crispr/Cas9 system in human iPSCs was first demonstrated by Mali and his colleagues in 2013 [109]. This study quantified indel mutations in PPP1R12C gene at AAV locus by next-generation sequencing. The indel mutation rate was found to be as 2.3% and 3.9% as a result of NHEJ mechanism [109]. Knowing that NHEJ occurs more frequently than HDR, the efficiency of Crispr/Cas9 is expected to be much lower in iPSCs.

Efficient and precise genome editing in iPSCs is based on HDR with a specific repair template. Gene disruption, on the other hand, is achieved via NHEJ mechanism. Accordingly, in case of monogenic diseases, genome-editing with a homologous repair template is desirable. Firth et al. produced iPSCs from cystic fibrosis patients carrying homozygous deletion of F508 in the *CFTR* gene[48]. Two methods were used in the generation of iPSCs. The first was transduction with 6-factor polycistronic lentiviruses which was later excised by Cre recombinase. The second was achieved by 4 individual Sendai viruses. The disease-specific iPSCs were then transfected with two separate plasmids expressing codon-optimized Cas9 and a gRNA hairpin. The functionality of gRNAs was validated both in HEK293 and iPSCs. The prominent aspect of the study was to accomplish footprint-free gene editing on the *CFRT* gene. Knowing that Cre recombinase leaves a genomic scar after excision, this study employed a piggyBac transposase to exclude additional sequences. Authors constructed a repair template with silent mutations creating *ClaI* site around the correction site and added pBac site together with a puromycin cassette. With this construct, they were able to select recombination of the repair template with puromycin. The integration efficiency of selected clones was found 16.7%. This study was important with its footprint-free gene-editing strategy, which would be useful in clinical applications[48].

Three groups have separately contributed to the gene correction in β-thalassemia patient iPSCs by using Crispr/Cas9 system. Each has focused on different mutations on *HBB* locus. One of the studies aimed to correct -28 (A/G) and 4-bp deletion at codon 41 and codon 42 of exon 2 [18]. Generation of patient iPSCs was through temperature-sensitive Sendai viruses containing OSKM. Three different gRNAs targeting HBB were tested in 293T cells for their functionality. As a repair template, the authors used piggyBac vector with neomycin cassette and both homology arms for *HBB* included 4-bp deleted sequence. The repair template was transfected into patient-derived iPSCs along with gRNA and Cas9 vector. Primers, one of which corresponded to piggyBac vector and the other corresponded to *HBB* outside the repair template, were designed to monitor HR-mediated correction. Out of 51 screened clones, 12 showed HDR corresponding to 23.5% efficiency. Similar to piggyBac vector used studies, piggyBac cassette was removed from corrected clones followed by negative selection with FIAU. Excision efficiency was calculated as 12.4%. 6 potential off-target sites similar to gRNA used for targeting were detected by BLAST search and these sites were analyzed by T7 Endonculease assay, which in turn showed no off-target effect. However, without whole genome sequencing, off-target effect has not been eliminated.

The other study has concentrated on 69A>T mutation in exon1 on *HBB* locus [51]. Differing than other studies, the authors generated iPSCs from adult hematopoietic cells by the transient expression of episomal oriP/EBNA-1 vector containing OSK and *Lin28*[119]. For gene targeting, designed gRNAs were cloned into Zero-blunt TOPO vector and human codon optimized Cas9 was used as a separate plasmid. Repair template comprised of HBB DNA template and PGK-*puro*-GFP cassette flanked by loxP sites. First, it was shown that one of the three gRNAs designed caused 3.5% indel by Illumina sequencing. Following selection with puromycin, PCR was used to detect targeted integration. Out of 10 clones screened, 4 of them showed HDR corresponding to 40% efficiency.

β-thalassemia patient iPSCs were also derived from patient fibroblasts carrying CD17 (A-T) homozygous mutation via polycistronic (OSKM) and excisable lentiviral system [52]. A single gRNA targeting HBB in the vicinity of point mutation and Cas9 plasmid were first tested in 293T cells, verified by T7E assay (43% indel rate). Repair template contained PGK-Hygromycin cassette flanked by loxP. Same as previous β-thalassemia studies, gene correction was detected by PCR. Out of 18 hygromycin resistant clones, 3 were shown to integrate the repair template. Direct sequencing also validated gene correction at the mutated site after excision of hygromycin cassette in three clones. Therefore, the targeting efficiency was calculated as 16.67% for Crispr-mediated gene editing.

One study compared TALENs and Crispr/Cas9 in terms of DSBs generation and homology-based integration in β-thalassemia derived-iPSCs [50] given that both strategies can target *HBB* locus [18], [52], [120]. Firstly, iPSCs were generated with oriP/EBNA-1 based pCEB4 episomal vector containing *Oct4*, *Sox2*, *Klf4*, *SV40LT* and *miR-302-367*. Hence, integration-free iPSCs were obtained. By using TALENs and Cas9/gRNAs, the authors tried to correct IVS2-654 C>T mutation. T7 endonuclease assay showed that Crispr/Cas9 gave rise to DSBs at a higher rate. To quantify HDR, they utilized piggyBac repair template with puromycin cassette. Primers, one of which corresponded to piggyBac vector and the other corresponded to *HBB* outside the repair template, were designed to monitor HR-mediated integration. In this case, TALENs were found to be more efficient than Crispr/Cas9 with 33% and 12.3% efficiency, respectively. Additionally, off-target effects were compared in 293T cells and patient iPSCs by T7 endonuclease assay. This assay showed more apparent indel formation in the cells transfected with Crispr components. Out of ten potential off-target sites, 7 of them were mutated in Crispr/Cas9 samples whereas 3 of them mutated in TALEN samples in patient iPSCs [50].

Crispr -mediated gene correction has been shown in dystrophin gene in Duchenne Muscular Dystrophy (DMD) patient iPSCs [61]. Dystrophin gene is located on X chromosome and the absence of exon 44 in mature mRNA causes DMD. In this study, three strategies were developed to restore the reading frame of the protein: exon 45 skipping, reading frame shift and exon 44 knock-in. First, 5' region of exon 45 was selected as a target site for which gRNAs and TALENs were designed. Among 15 pairs of TALENs and 5 gRNAs, the ones with highest cleavage activity were selected with a *XcmI* sensitivity assay. TALEN and gRNA1 gave similar mutagenesis rates. To generate exon 44 knock-in, the authors designed a donor template containing silent mutations at the nuclease-targeting site in exon 45 and a hygromycin cassette flanked by *loxP* sites. After hygromycin selection and limiting dilution, clones were analyzed by PCR. TALEN-mediated clones showed %95 efficiency whereas Crispr-mediated clones had 75% recombination. Southern blot confirmed single-copy knockin with 87% and 50% efficiency in TALEN- and Crispr-mediated samples, respectively. Cre recombinase excised hygromycin cassette with 60% and 65% in TALEN- and Crispr-mediated knockin experiments. Finally, T7E assay and amplicon deep sequencing were applied on corrected clones to detect rare mutations at the target site. No increased mutation rate was observed. Additionally, G-band for karyotyping, SNP array for detecting CNVs and exome sequencing for SNVs and small indels were employed all of which showed no additional aberrations. This study underscores the combination of various methods for off-target mutagenesis for gene therapy.

1.3. Familial Mediterranean Fever

Familial Mediterranean Fever (FMF) is a hereditary autosomal recessive autoinflammatory disease, characterized by recurrent fever and pain in abdomen, chest or joints[121]. It is primarily observed in Middle Eastern populations such as Sephardic Jews, Armenian, Turkish and Arabian descendants. It is caused by missense mutations in the *MEFV* gene encoding pyrin protein which is a regulatory protein in inflammation. *MEFV* is located on chromosome 16. Over 80 mutations have been identified in the literature [122]. The majority of the mutations is clustered in exon10 (**Figure 3**) and the most common are M694V, M680I, M694I and V726A, accounting for 80 % of FMF cases in the Middle East [123].

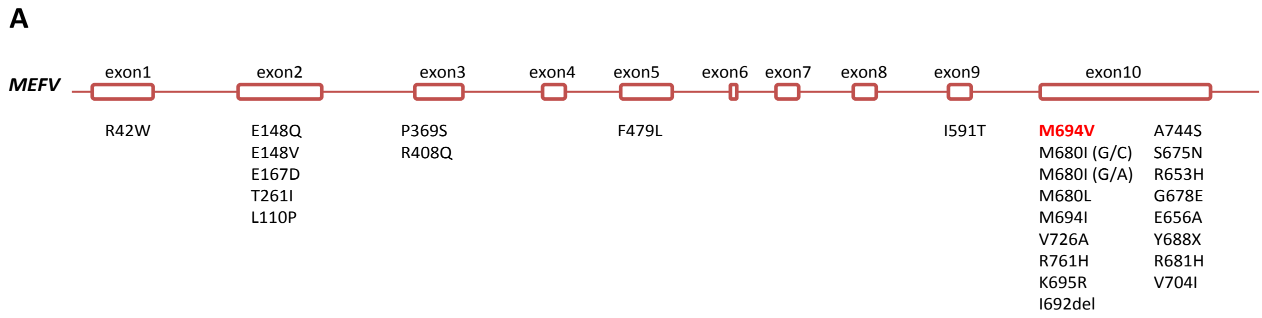

Figure 3. The distribution of MEFV mutations and the domains of pyrin protein (Adapted from [124])

Prevalence of mutation differs in various populations. For example, in Turkish population, M649V is most prevalent followed by M680I and V726A [125]. Some studies indicate that M694V homozygous patients undergo a more severe form of the disease [125]. Amyloidosis, which is the most serious complication in FMF, has been reported in such patients more frequently. However, a relationship between a mutation and the age of onset of the disease has not been clearly identified [126].

MEFV was found to be expressed in mature neutrophils and macrophages. The prepromyelocyctic cell line HL60 expresses *MEFV* at granulocyctic and monocyctic differention. It is also expressed in monocyctic cell lines such as U937 and THP-1 [127]. Pyrin encoded by *MEFV* plays role IL-1β processing, NF-κB activation and apoptosis [121]. Mutated pyrin causes abnormalities in inflammation. Pyrin, also called marenostrin, involves a novel protein domain called Pyrin domain (PYD) at the N-terminal and it belongs to the death domain fold family [128]. PYD domain has been suggested to interact with apoptosis-associated speck-like protein (ASC) and regulate NF-κB activation[129]. Pyrin also comprises of b-Zip, B-Box, coiled-coil and a C- terminal B30.2 domains. C-terminal B30.2 domain, on the other hand, has been reported to interact with caspase-1 to modulate IL-1β [130]. It is also important to note that the M694V mutation resides in B30.2 domain.

Studies showed that pyrin regulates the IL-1β, pro-inflammatory cytokine [129]. Impaired pyrin has been speculated to play role in NLRP3 inflammasomes [128]. Inflammasomes are cytosolic multiprotein complexes responsible for the maturation of proinflammatory cytokine such as IL-1β.

Elevated IL-1β level is one the disease-related phenotypes of FMF patients. IL-1β is translated as pro protein to be cleaved by cysteine-aspartic acid protease caspase-1 [131]. Activity of caspase-1 is self-regulatory as well as affected by other mechanisms. Caspase-1 activation occurs upon signaling by danger-associated molecular patterns (DAMPs) and pathogen-associated molecular pattern (PAMPs)[131]. The signaling assembles inflammasomes which consist of Nod-Like receptor subfamily NLRP3 containing PYD domain, adaptor protein ASC and caspase-1 [131][132]. Pyrin has been thought to regulate inflammasome assembly as a negative modulator. However, there are a discrepancies between the studies where Pyrin has been shown to either increase IL- 1β secretion or diminish it[128][130]. As such, the exact role of the Pyrin mutations in yet fully elucidated. In order to facilitate research on understanding the disease mechanisms of FMF, cell lines that harbor particular *mefv* mutations and their genetically matched controls are needed. Towards this goal, we have recently described the generation of iPSCs from a patient harboring homozygous M694V mutation in the *mefv* gene[133].

CHAPTER 2

MATERIALS AND METHODS

2.1. Maintenance and expansion of human iPSCs

FMF patient iPSCs were cultured with mTeSR1 or E8 medium on tissue culture plates coated with Matrigel or Vitronectin, respectively. Accutase (Sigma) for 5 minutes at 37^{0}C was used for the detachment of the cells cultured in mTeSR1. The cells were collected with Dulbecco's modified Eagle's medium (DMEM F12) and centrifuged at 1000rpm for 2 minutes. They were plated with fresh mTeSR1 supplemented with 10 μM ROCK inhibitor Y-27632 during the first 24 hours. PBS EDTA was used to detach cells cultured in E8 medium. After washing two times with PBS-EDTA, cells were incubated PBS-EDTA for 3 minutes at 37^{0}C. Then, PBS-EDTA was carefully aspirated and the cells were collected with DMEM F12 to be centrifuged at 1000rpm for 2 minutes. Fresh E8 medium was slowly added to obtain clumps and those were plated on vitronectin-coated plates. The cells were passaged every 5 days. All cells were maintained on 6-well plates at 37^{0}C and 5% CO_2 in a humidified incubator.

2.2. Design and cloning of sgRNAs and *mefv* repair template

100bp *mefv* sequence was chosen at the vicinity of M694V mutation on *mefv* gene at position 16p13.3 as a target sequence. sgRNAs with highest score in CRISPR design tool [134]were directly ordered to be synthesized and cloned into PX459 vector and PX330 (Addgene #48139 and #58782). Plasmids were digested by *BbsI* for 1 hour at 37^{0}C and treated with Antarctic Phosphatase (NEB, UK) and 10X AP Buffer for another 15 minutes at 37^{0}C. Synthesized top and bottom oligos (100μM of each) were annealed and phosphorylated with 10X T4 Ligation Buffer (NEB), T4 PNK (NEB) using a themocycler with the following parameters: 37^{0}C for 30 minutes and 95^{0}C for 5 minutes then ramping down to 25^{0}C at 5^{0}C /minute. Annealed and phosphorylated oligos were 1:200 diluted, of which 1μl was used in ligation reaction with *BbsI*-digested PX459 or PX330. For ligation, Quick Ligation Kit (NEB, UK) was used. Digested and AP-treated vector alone was used as a control. 5 μl of ligation reaction was transformed into competent bacteria. Successful clones were confirmed by sequencing. 80bp GFP single strand oligodeoxynucleotides (ssODNs) were ordered from IDT to be used in GFP reporter assay. Truncated GFP vector (tGFP) (Addgene #26864) was linearized with *XbaI* at 37^{0}C for 1 hour. tGFP was also used to detect homologous recombination rate in GFP reporter assay.

As a *mefv* repair template, 760bp *mefv* fragment covering M694V was PCR amplified with the following conditions: 98^{0}C 30 sec, 98^{0}C 10 sec, 64^{0}C 30 sec, 72^{0}C 45 sec, 34 cycles and PCR purified with NucleoSpin® Gel and PCR Clean-up Kit (Macherey-Nagel, Germany) and cloned into pCR4-TOPO vector. Silent mutation and *RsaI* restriction site were introduced into *mefv* repair template by site directed mutagenesis. (NEB Q5® Site-Directed Mutagenesis Kit. At the first step of site directed mutagenesis 25ng of pCR4-TOPO vector was PCR amplified with site directed mutagenesis primers using the following conditions: 98^{0}C 30 seconds, 98^{0}C 10 seconds, 65^{0}C (seed sequence silent mutation) 69^{0}C (*RsaI* site mutation) 30 seconds, 72^{0}C 2 minutes, 4^{0}C hold. 1µl of PCR product was KLD treated with 2X KLD Reaction Buffer, 10X KLD Enzyme Mix and nuclease-free water at room temperature for 5 minutes. 5 µl of KLD reaction was transformed into NEB 5-alpha Competent *E.coli*. Colony picking followed by inoculation and mini-prep (MN, Germany) were confirmed by sequencing. Selected clones were DNA purified with NucleoBond® Xtra Maxi EF (MN, Germany) and linearized with *XmnI*.

180bp *mefv* antisense wild type and mutant ssODNs were ordered from IDT to be used in HR.

Table 2. *mefv* exon10 targeting gRNAs

gRNAs targeting *mefv* exon10	**Sequence**
gRNA1	CACCGTCGCCAGAGAATGGCTACT
gRNA2	CACCGTGTCGCCAGAGAATGGCTAC
gRNA3	CACCGACCACCCAGTAGCCATTCTC
gRNA4	CACCGCCTGCTTATGGATGTCTTGC

Table 3. List of primers for *mefv* exon 10 amplification, repair template design and T7 endonuclease assay

Primers	Sequence
E10U2- F (mefv exon10)	TGCATTTCCCATAGCAGCTA
E10D1- R (mefv exon10)	TTCCAGAAGAACTACCCTGT
F_mefv_100bp fragment	TTATCGTCTAGAGGGAGCCTGCAAGACATCCA
R_mefv_100bp fragment	ATTTAGGCGCGCCTTTATTAGCAGGCGGTCGG
Q5_fwd_seed_e10g2	CAGAGAATGGTTATTGGGTGG
Q5_rev_seed_e10g2	GCGACAGAGTCATGTTCCCTT
Q5_RsaI_fwd	CTGGCCGCCGGTACTGGGAGG
Q5_RsaI_rev	AGAGGAAACTCGGAGAGCCC
T7E_e10g2_fwd	CTACCCTGTCCCTGTTTCCTG
T7E_e10g2_rev	AGAGCAGCTGGCGAATGTAT
fwd_mefv_e1_50	ACCCCTAGTGACCATCTGCT
rev_mefv_e1_620	TGCTAACCTAGAGATGTTTGTCTGA
M694V_common_F	CCCAACCTCATCTTCTCTGATGATCTGA
M694V_common_R	CAGAGAAAGAGCAGCTGGCGAATGTATA
M694V_M	AGAATGGCTACTGGGTGGTGATAAGGG
M694V_V	TGGACGCCTGGTACTCATTTTCCTTAAT

2.3. Generation of 293T cells stably expressing GFP

pEGIP lentiviral vector (Addgene #26777) stably expressing GFP with puromycin cassette was packaged using Human Embryonic Kidney cells (HEK, 293Ts). Viral production was performed by the liposomal transfection of transfer vector (pEGIP), envelope vector (VSV-G) and packaging vector (VPR-Δ8.2) into 293T cells. $2.5x10^6$ cells were seeded on 10cm-plates at day 0 with DMEM with 10% FBS and 1% penicillin/streptomycin (D10 medium). Next day, they were transfected with 2.5μg pEGIP, 2.25 μg VPR-Δ8.2 and 2.5 μg VSV-G using FuGENE® HD Transfection Reagent (Roche, Switzerland). At day 2, fresh D10 medium was added on the plates. 48h and 72h post transfections, media was collected and filtered (0.45μm). Viruses were collected in medium were aliquoted in 1ml and stored at -80^{o}C.

200,000 293T cells were seeded on 6-well plates one day prior to transduction and transduced with 0.5ml of pEGIP containing fresh DMEM+10% FBS supplemented with 10μg/ml protamine sulfate. 16h post transduction, medium was replaced with fresh D10 medium. The cells were puromycin selected for 3 days (D2-D5).

2.4.Generation of EGFP-deficient 293T cells

pEGIP*35 lentiviral vector (Addgene #26776) involving a stop codon, HindIII site and a successive intervening sequence in EGFP sequence was packaged with 293T cells. Same as with pEGIP,viral production was performed by the liposomal transfection of transfer vector (pEGIP), envelope vector (VSV-G) and packaging vector (VPR-Δ8.2) into 293T cells. $2.5x10^6$ cells were seeded on 10cm-plates at day 0 with DMEM with 10% FBS and 1% penicillin/streptomycin (D10 medium). Next day, they were transfected with 2.5µg pEGIP, 2.25 µg VPR-Δ8.2 and 2.5 µg VSV-G using FuGENE® HD Transfection Reagent (Roche, Switzerland). At day 2, fresh D10 medium was added on the plates. 48h and 72h post transfections, media was collected and filtered (0.45µm). Viruses were collected in medium were aliquoted in 1ml and stored at -80^{0}C.

200,000 293T cells were seeded on 6-well plates one day prior to transduction and transduced with 0.5ml of pEGIP containing fresh DMEM+10% FBS supplemented with 10µg/ml protamine sulfate. 16h post transduction, medium was replaced with fresh D10 medium. The cells were puromycin selected for 3 days (D2-D5).

2.5. Generation of pegip-mefv-100bp construct

The target site encompassing M694V mutation in mefv sequence to design gRNAs was 100bp in length. This sequence was amplified by PCR by using specific primers, each of which contained *XbaI* or *AscI* restriction site at their 5' site. The following condition was used for amplification: 95^{0}C 3 min, 95^{0}C 30 sec, 57.5^{0}C 30 sec, 72^{0}C 30 sec x 35 cycles and PCR product was run on 2% agarose gel. Gel extraction was done with NucleoSpin® Gel and PCR Clean-up Kit (Macherey-Nagel, Germany) and resulting 100bp fragment was digested with *AscI* and *XbaI* to get proper overhangs at 37^{0}C for 1 hour. Digestion product was PCR purified with the same kit. pEGIP-mefv-crispr_clone7 vector DNA in which *XbaI* and *AscI*, sites were previously constructed by Dr. Tamer Önder was digested with *XbaI* and *AscI* at 37^{0}C for 1 hour and treated with AP at 37^{0}C for 15 min. AP was inhibited at 70^{0}C for 5 minutes. 4.5 ng of insert was used for 50 ng vector DNA in ligation reaction at RT for 10 minutes with Quick Ligation Kit (NEB, UK). 5 µl of ligation reaction was transformed into 50 µl competent DH5α. Successful clones were first checked with double digestion with *XbaI* and *AscI* and further confirmed by sequencing. 2.5 µg Pegip-mefv-100bp construct was transfected with envelope vector (VSV-G) and packaging vector (VPR-Δ8.2) using FuGENE® HD Transfection Reagent (Roche, Switzerland) into $2.5x10^6$ 293T cells on 10-cm plates seeded 1 day before. At day 2, fresh D10 medium was added on the plates. 48h and 72h post transfections, media was collected and filtered (0.45µm). Viruses were collected in medium were aliquoted in 1ml to be stored at -80^0C. $1x\ 10^6$ 293T cells were seeded on 6-cm plates. Those cells were infected with pEGIP-mefv-100bp virus at MOI:10 , MOI:1 and MOI:0.1 with 8 µg protamine sulfate (Sigma-Aldrich). Next day, fresh D10 was added into plates subsequent to aspiration of the older. At day 2, puromycin selection started and majority of infected cells with MOI:0.1 were dead at the end of the 3^{rd} day. Those cells were expected to have single or double integration site, therefore they were expanded to be used for testing *mefv*-targeting gRNAs.

2.6. Transfection of 293T cells and FMF patient iPSCs

200,000 293T cells were seeded on 6-well plates one day prior to transfection. FuGENE® HD Transfection Reagent along with DMEM was used to transfect 1 µg PX459 and/or 1 µg linearized tGFP or GFP ssODNs. FUtdTW (Addgene #22478) vector was used as a transfection control. DNA:FuGENE ratio was determined as 1:3. FuGENE+DMEM and DNA+DMEM mixtures were prepared separately and later added on each other. Final FuGENE+DNA mixture was incubated at room temperate for 30 minutes and added on 293T cells dropwise.

Nucleofection of iPSCs were achieved by Amaxa 4D-Nucleofector X unit (Lonza). FMF patient iPSCs cultured on conditioned medium on Matrigel-coated 6-well plates were treated with 10 µM ROCK inhibitor (Y-27632) overnight one day prior to nucleofection. At the day of nucleofection 12-well plates were coated with Matrigel and kept at room temperature 1h before nucleofection, one well for each nucleofection reaction. Additional mTeSR1 supplemented with 10 µM ROCK inhibitor was prepared. 1ml of pre-warmed mTeSR1 with ROCK inhibitor was added on each well after aspirating DMEM F12 in Matrigel-coated 12-well plates. For each nucleofection reaction, $0.5\text{-}2x10^6$ cells were used. $0.5x10^6$ cells were most frequently used in our experiments for a single cuvette. mTeSR1 with ROCK inhibitor was removed from the plates and FMF patient iPSCs were disassociated with Accutase at 37^0C for 5-8 minutes and gently collected with DMEM. By pipeting up and down, single cell suspension was obtained and centrifuged at 1000rpm for 2 minutes. The cells were resuspended in mTeSR1 with ROCK inhibitor and counted. Required number of cells was collected separated and centrifuged again at 1000rpm for 2 minutes. The cells were resuspended pre-warmed P3 Primary Cell Solution. 1 μg PX459 (containing Cas9 and gRNA), 1 μg *mefv r*epair template or 1 μl mefv ssODN (10 μM) were dissolved in P3 Primary Cell Solution. The concentration of the plasmids was arranged so that the volume of the total DNA did not exceed 1/10 of the reaction volume (10μl for 100 μl nucleocuvette). Therefore, the cells were resuspended in 80 μl whereas the DNA mixtures were prepared in 20 μl solutions. They were added in each other for each nucleofection reaction and transferred to 100 μl single nucleocuvette which was placed into Amaxa Nucleofector. Program CB-150 was run for nucleofection of iPSCs. After the reaction, 400 μl warm mTeSR1 with ROCK inhibitor was added to the nucleocuvettes and each reaction was transferred into Matrigel-coated 12-well plate avoiding frequent pipetting up and down. 24h post transfection, cells were checked for attachment and medium was replaced with fresh mTeSR1. 48h post nucleofection, 0.5 μg/ml puromycin was added to start the selection process which continued approximately for 6 days (until untransfected controls all died). 1 μg pmax-GFP and 1 μg pEGIP plasmid were both used as positive controls for nucleofections.

2.7. Surveyor Nuclease Assay

293T cells in 6-well plates were harvested for genomic DNA extraction. First, D10 medium (DMEM+10% FBS+1% penicillin/streptomycin) was aspirated. Upon trypsin addition, the cells were disassociated at 37^0C after 3 minutes. The cells were collected with the same amount of D10 and centrifuged at 1500rpm for 5 minutes. Cell pellets were resuspended in 1X PBS (Hyclone) and centrifuged at 300 rpm for 3 minutes. DNA isolation was achieved by NucleoSpin® Tissue kit (MN, Germany). DNA concentrations were measured in nanodrop. 50ng/μl template DNA was used for amplification. 760bp sequence around M694V mutation in exon10 of *mefv* locus was PCR amplified with Surveyor primers (see Table I) using Phusion® High-Fidelity DNA Polymerase (NEB). The conditions were as follows: 98^0C for 30 seconds, 98^0C for 10 seconds, 64^0C for 30 seconds, 72^0C for 45 seconds, (34 cycles) 72^0C for 5 minutes, 4^0C hold. 5 μl of 50 μl reaction was run in 1.0% agarose gel to detect single DNA band. 200-400ng of PCR product was used for heteroduplex formation using a thermocycler. The program for hybridization is shown in Table II. 18 μl of hybridized PCR product was treated with 0.15M $MgCl_2$, 1 μl Surveyor Nuclease at 42^0C for 1 hour. 2.2 μl ($1/10^{th}$ of final volume) Stop Solution was used at the end of the reaction. (The amounts were determined based on control experiments in which control plasmids of the kit were used). The digestion products were run on 2% agarose gel and analyzed.

2.8. Amplification-Refractory Mutation System

Amplificaton- Refractory Mutation System (ARMS) utilizes multiple primers in a single PCR reaction for genotyping wild type and mutant alleles in samples. ARMS primers for mutant and wild type *MEFV* alleles were designed as indicated in **Figure 4**. (**Table 3**)

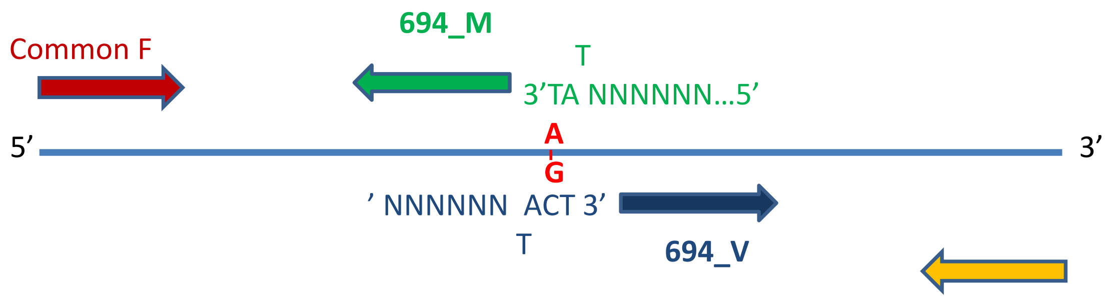

Figure 4. Design of ARMS PCR primers for wild type and mutant MEFV alleles.

Genomic DNA was isolated from dH1fs, 293Ts, FMF patient and parent iPSCs, Using 50ng template DNA, PCR amplification was done by the following conditions: 94^{0}C 5 min, 65^{0}C 30 s, 72^{0}C 25s for 33 cycles, a final extension step at 72^{0}C for 10 min. 15µl of PCR product was run on 2% agarose gel and visualized.

2.9. Single cell isolation of 293T and THP-1 cells

In order to seed 293T cells into 96-well plates they were first trypsinized and centrifuged at 1500 rpm for 5 minutes. They were resuspended in D10 medium and counted. Limiting dilution was applied to obtain 1 cell in 100 µl D10 medium. The cells in 96-well plates were monitored for 2 weeks and the colonies started to form at the end of 2 weeks during which 100 µl fresh D10 was added once. The wells with colonies were marked for DNA isolation and further expanded.

96-well plate was quickly inverted to dump media and remove the excess liquid by blotting on paper towels. The cells were washed with 1X PBS 150 µl. 50 µl Bradley Lysis buffer containing Proteinase K was added to each well. The lid of the plate was replaced and sealed with parafilm. The plate was placed into humidified chamber at 60^{0}C overnight. Next it was cooled down to RT and 100 µl ice-cold EtOH/NaCl mix was added to precipitate DNA. The plate was incubated at RT for 30 minutes and then centrifuged at 3000rpm for 20 minutes and inverted to decant the liquid. 150 µl cold 70% EtOH was added and the plate was centrifuged at 2000rpm for 10 minutes. The pellet was rinsed and supernatant was decanted. Washing step was repeated until there is no detectable EtOH. Finally, 30 µl warm TE (pH 8.0) was added and the plate was covered with parafilm and incubated at 56^0C for 10 minutes.

THP-1 cells were seeded on 96-wells in the same way. The appearance of colonies in 96-well plate took approximately 3 weeks. After they grew, they were transferred to 48-well plates and 24-well plates, respectively. The cells were 24-well plates were transferred to eppendorf tubes and DNA isolation procedure was applied.

2.10. Flow Cytometry

Transfected 293T cells were treated with trypsin and incubated at 37^0C for 5 minutes. Pre-warmed D10 was added on dissociated 293T cells to be collected. The cells were transferred to flow cytometry tubes and centrifuged at 1500 rpm for 5 minutes. The medium was aspirated and the pellet was resuspended in 1X PBS 1% FBS solution. Resuspended cells were placed onto ice. BD Accuri C6 Flow Cytometer (BD Biosciences) was used to analyze the samples according to the manufacturer's instructions.

Table 4. List of vectors and their corresponding figures

Vector	Function	Important feature	Figure
hCas9	Expresses human codon optimized Cas9		6C,7B
pX330	Expresses Cas9&gRNA	Cloning vector for T1 and T2 gRNAs	6C,7B
FUtdTW	Expresses fluorescence protein	Transfection control	6D
pX459	Expresses Cas9&gRNA	Cloning vector for EGFP- (T1&T2) and MEFV-targeting gRNAs (G1-G4),enables puromycin selection	6E, 8A, 8B, 9A, 9B, 10B, 10C
tGFP	Truncated GFP expression	EGFP donor template	8A,9A, 9B
pEGIP	Stably integrates EGFP	Lentiviral backbone, puromycin selection	6A
pEGIP*35	Stably integrates mutant EGFP	Assessing HR-mediated gene targeting efficiency for gRNAs T1&T2	7A
pEGIP-100bp-mefv	Stably integrates EGFP disrupted by 100bp *mefv* sequence	Assessing HR-mediated gene targeting efficiency for gRNAs (G1-G4)	8A, 9A, 9B
pCR4-TOPO-mefv	*MEFV* repair template	Silent mutations around PAMs, *RsaI* site	13
pmax-GFP	Expresses EGFP	Nucleofection control	11
lentiCRISPR v1	Stably expresses Cas9&gRNAs	Lentiviral backbone, puromycin selection, cloning vector for mefv exon1 gRNAs	A1B, A1C

CHAPTER 3

RESULTS

3.1. Validation of M694V mutation in both fibroblasts and iPSCs by sequencing

DNA samples from an FMF patient and their parent skin fibroblasts were sequenced to pinpoint the M964V mutation to be corrected. Accordingly, FMF Patient- and parent-derived iPSCs sequencing data confirmed M694V mutation. As a control, skin fibroblasts from a healthy donor was used which was homozygous wild type **(Figure 5A)**. Both FMF patient fibroblasts and iPSCs sequencing revealed that they were homozygous for mutant A>G allele. Parent fibroblasts and iPSCs were heterozygous for mutant A>G allele according to sequencing data **(Figure 5B)**.

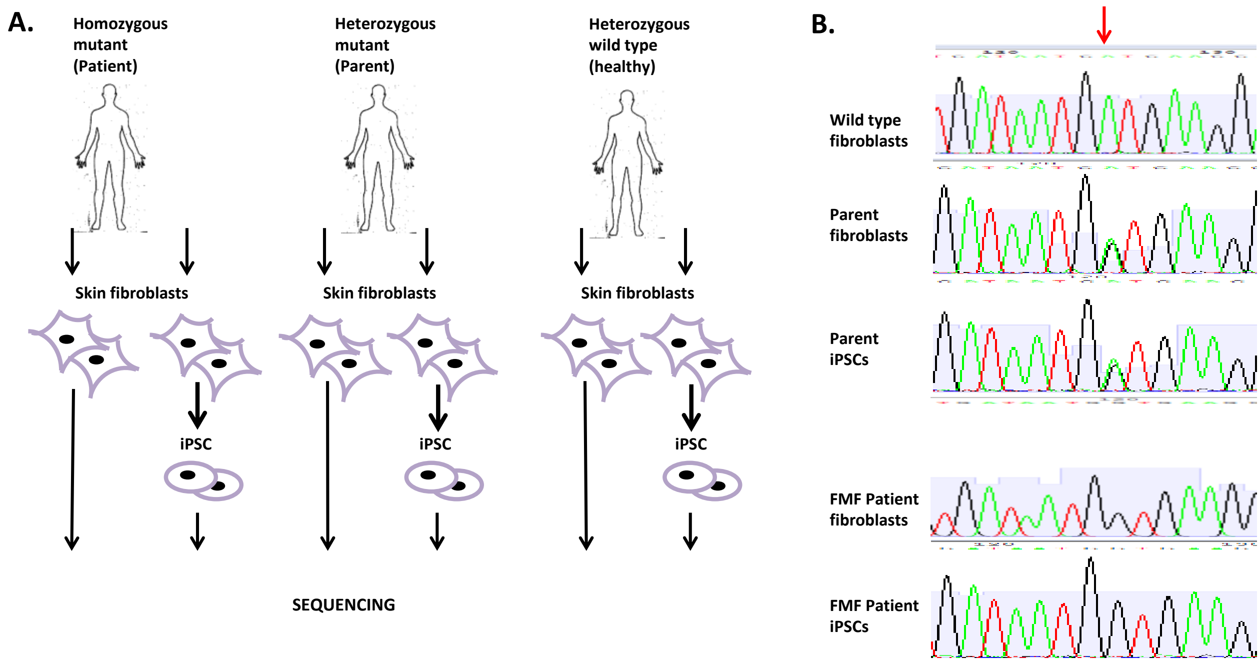

Figure 5. The validation of M694V mutation in both fibroblasts and iPSCs by sequencing. (a) The skin fibroblasts taken from an FMF patient, parent and a healthy individual were reprogrammed into iPSCs. Both fibroblasts and iPSCs were sequenced to pinpoint M694V mutation in all samples. (b) The location of the disease associated mutation (red arrow) as revealed by sanger sequencing in patient, parent and healthy samples, respectively.

3.2. Characterization of iPSCs derived from FMF patients

Primary fibroblasts cultures from a patient diagnosed with FMF and his parent were obtained by skin biopsy. The primary fibroblasts were reprogrammed into iPSCs with episomal vectors (Materials and Methods). iPSC clones were expanded **(Figure 6A).** The expanded clones were injected into immunosuppressed mice and formed tumors containing different cell types that represent three germ layers **(Figure 6B)**. The clones were checked for pluripotency markers (Oct4, Nanog, SSEA-4). All three clones of FMF patient-, parent- and PBMC iPSCs expressed pluripotency markers **(Figure 6C)**. FMF Patient- and parent-derived iPSCs retained pluripotency, differentiation into three germ layers and could form teratomas [133].

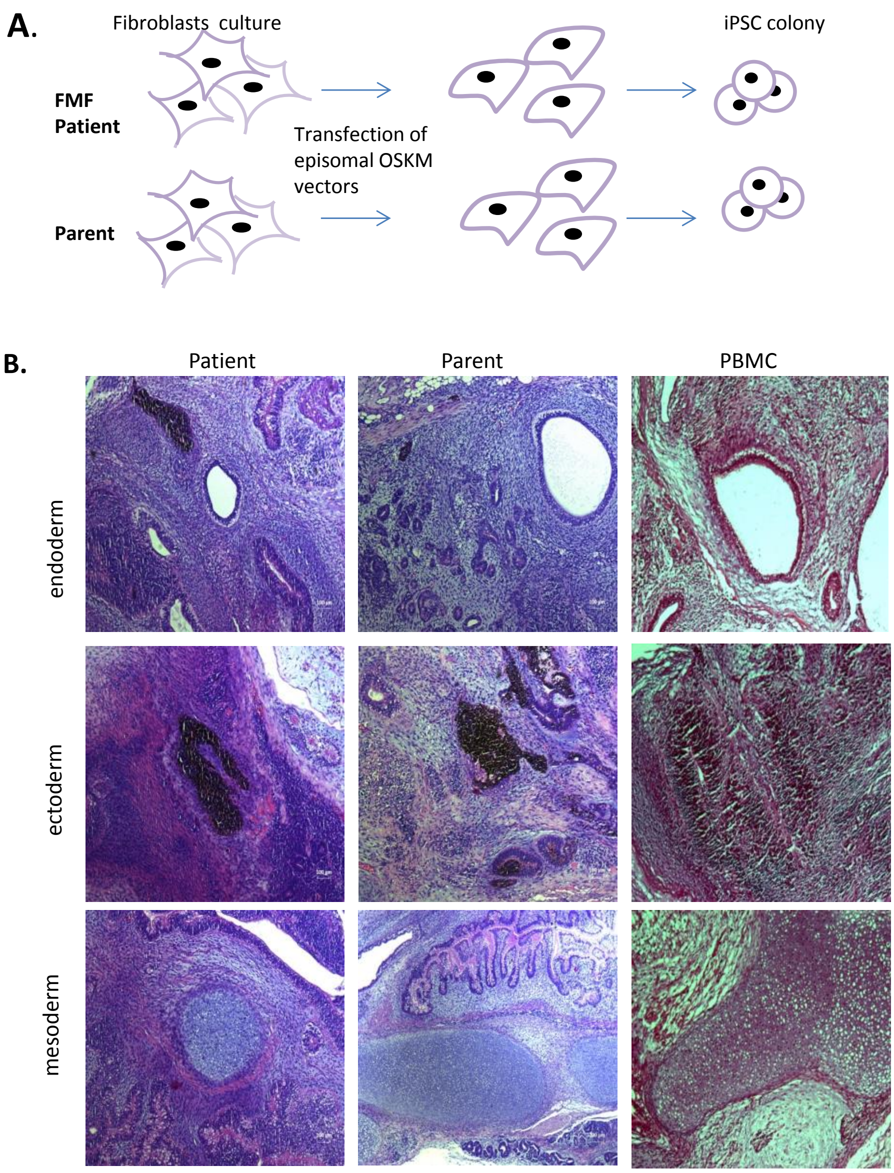

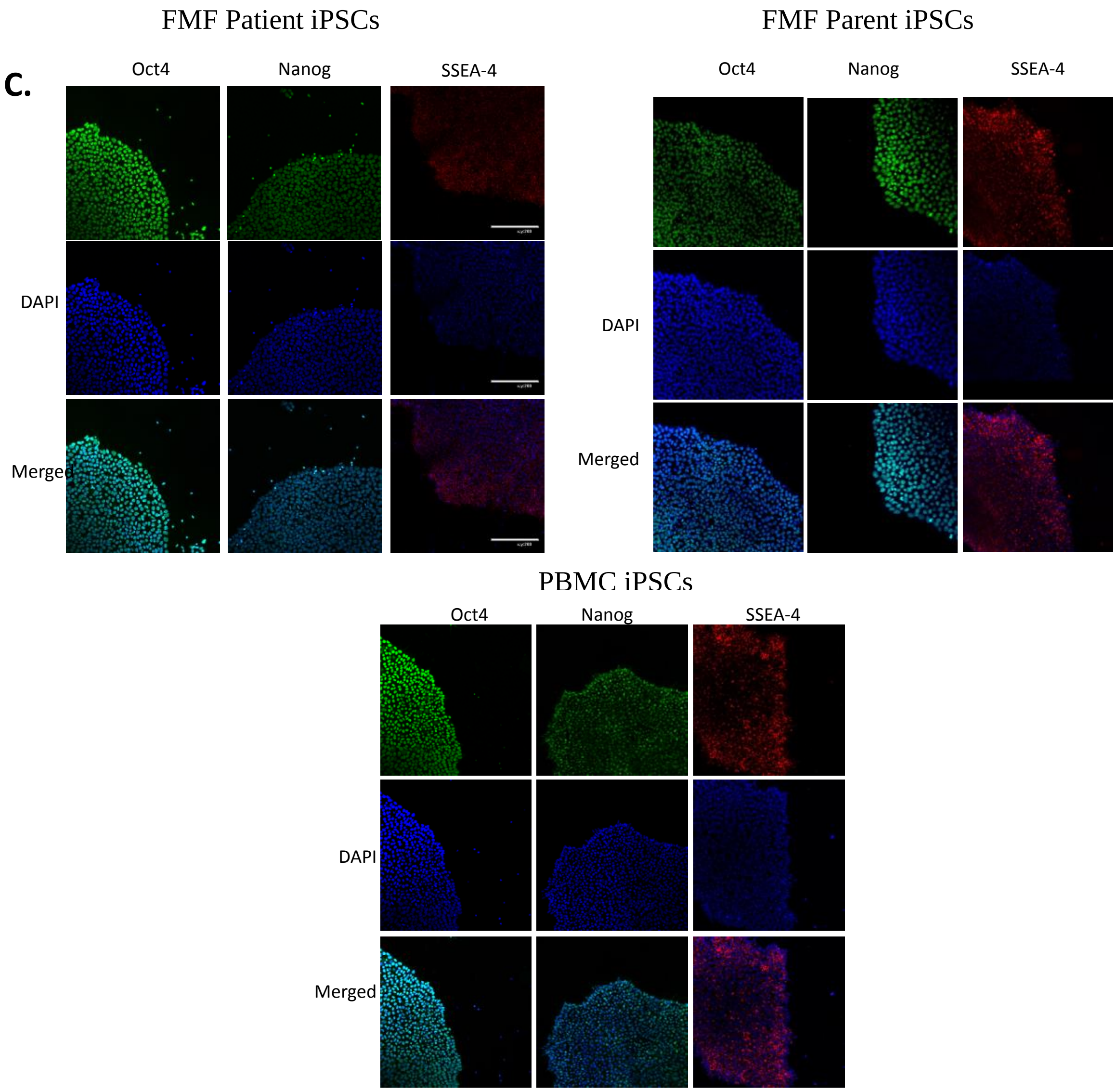

Figure 6. Characterization of iPSCs derived from FMF patients and parent iPSCs.
(a) Parent and patient fibroblasts were reprogrammed into iPSCs by the transfection of episomal *Oct-4, Sox2, Klf4* and *c-myc* vectors. (b) Characterization of teratomas formed by FMF patient, parent and PBMC iPSCs. Three germ-layers for each sample were shown. (c) Immunofluorescence staining of Oct-4, Nanog and SSEA-4 proteins in FMF patient, parent and PBMC iPSCs. (Green for Oct-4 and Nanog, Hoecsht for nucleus, red for SSEA-4)

3.3. Generation of a reporter system to assay Crispr/Cas9 components for DSB

In order to confirm the functionality of CRISPR components, a reporter system was established with stably GFP-expressing 293T cells. pEGIP vector contained puromycin cassette enabling selection after transduction **(Figure 7A)**. The system began with the transduction of 293T cells with pEGIP vector and followed by puromycin selection. Transduction of the PEGIP vector was performed at an MOI of 0.3 to generate single copy integrants which were established as a cell line. Upon transfection of Cas9 and EGFP-targeting sgRNAs T1 and T2, GFP expression was monitored by flow cytometry at day 3. As a transfection control Tdtomato was used. The samples which expressed Cas9 and one of the EGFP-targeting sgRNAs together showed a significant increase (17.7% and 11.7%) in GFP-negative cells compared to controls. **(Figure 7B-D)**. Later, pX459 plasmid which expressed both Cas9 and sgRNAs was used in the same system and the increase in GFP-negative cells were analyzed at 3-day intervals **(Figure 7E)**. The increase in GFP-negative cells were higher in sgRNA T1-expressing samples than those of sgRNA T2-expressing ones. These results concluded that EGFP-targeting sgRNAs and Cas9 were functional and cause double-stranded breaks in the cell.

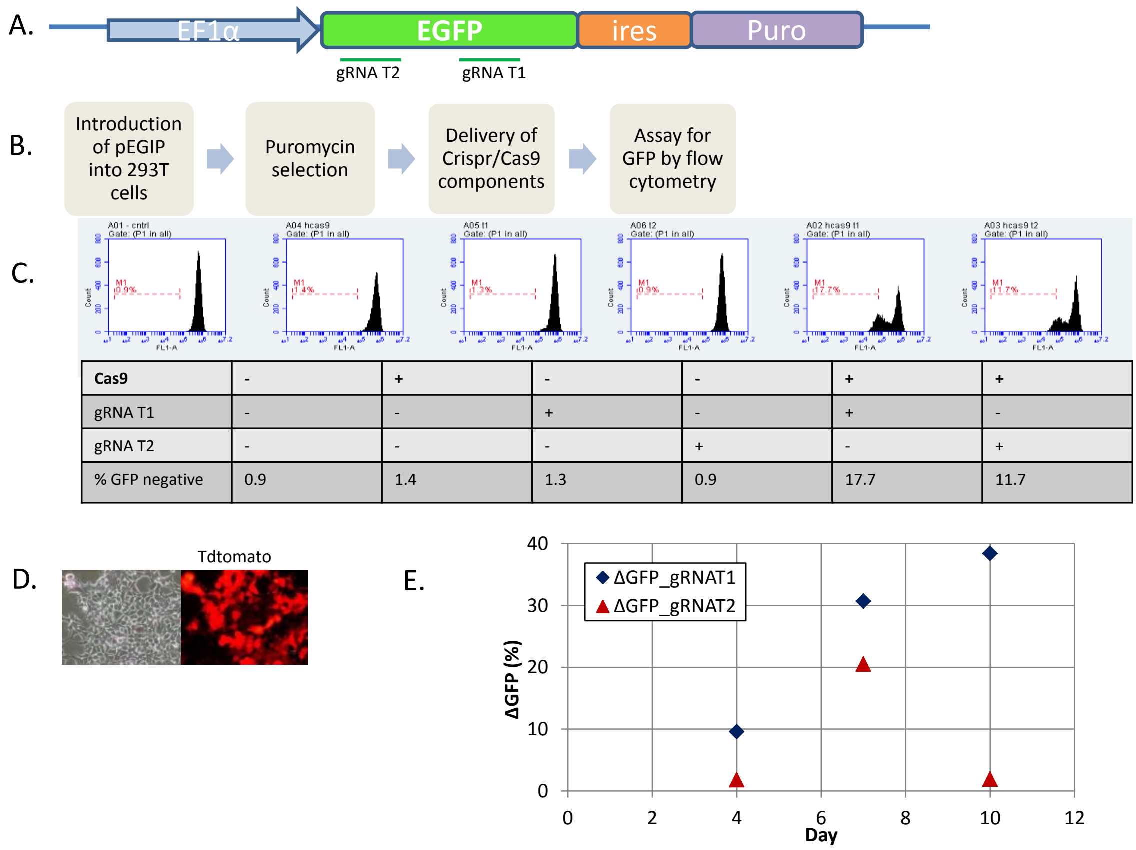

Cas9	-	+	-	-	+	+
gRNA T1	-	-	+	-	+	-
gRNA T2	-	-	-	+	-	+
% GFP negative	0.9	1.4	1.3	0.9	17.7	11.7

Figure 7. Generation of a reporter system to assay to Crispr/Cas9 components for DSB.
(a) Schematic representation of pEGIP vector. sgRNAs targeting EGFP sequence (gRNAT1 & T2) are underlined. (b) Flowchart for the GFP analysis in 293T cells by flow cytometry. (c) Percent GFP (-) cells in different conditions. (d) Positive control for liposomal transfection with Tdtomato vector. (e) Time-course change in GFP expression in GFP-expressing 293T cells after transfection with pX459-T1/T2 vector. (no puromycin selection)

3.4. GFP reporter assay confirmed homologous recombination in 293T cells

Knowing that Cas9 and EGFP sgRNAs can generate indels in 293T cells, we needed to further demonstrate that EGFP phenotype could be restored in 293T cells by Crispr/Cas9 system when repair template was supplied. For this purpose, we used pEGIP*35 vector in which EGFP sequences was disrupted by a stop codon and an intervening sequence. After the transduction of 293T cells with the vector, we selected the EGFP mutant 293Ts with puromycin and checked if EGFP was restored when they were transfected with Cas9 and sgRNA T2 plasmids together with ssODNs for EGFP. Both GFP-antisense and sense strands were used to compare HR efficiencies **(Figure 8A)**. Flow cytometry showed the appearance of GFP-positive cells in the samples containing repair template. GFP-antisense strand appeared to be slightly more efficient than GFP-sense template with 0.5% GFP percentage **(Figure 8B)**. The images of EGFP-corrected and mutant 293Ts could be seen in **Figure 8C**.

A.

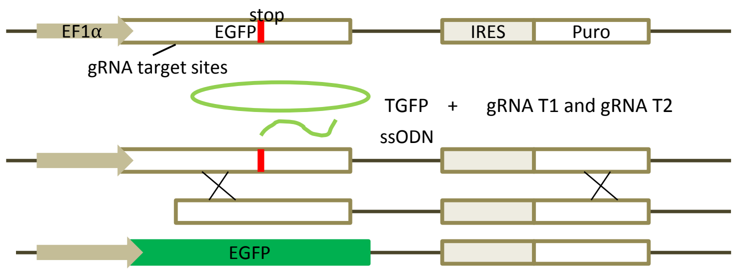

B.

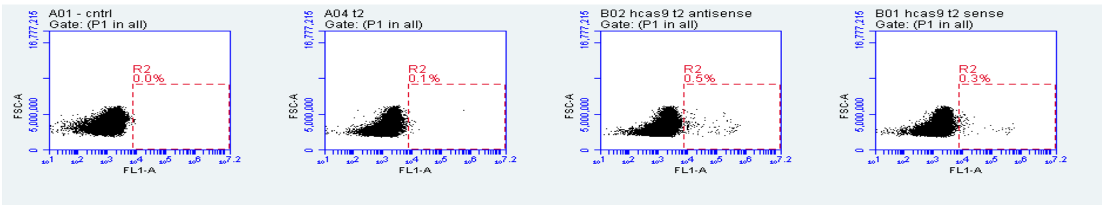

Cas9	-	-	+	+
gRNA T2	-	+	+	+
ssODN sense	-	-	-	+
ssODN antisense	-	-	+	-
% GFP positive	0.0	0.1	0.5	0.3

C.

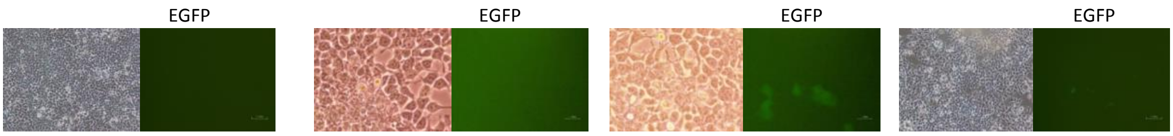

Figure 8. GFP reporter assay to monitor homologous recombination.
(a) Schematic representation of pEGIP*35 vector and the strategy used for Crispr/Cas9-mediated homologous recombination in 293T cells. Double-stranded truncated GFP vector (TGFP) and single-stranded GFP oligos were used as donor templates. (b) Percent of GFP-expressing cells was shown by flow cytometry. (c) GFP expression in transfected 293T cells. (gRNA T1 and gRNA T2 is 33bp and 23 bp apart from the mutant site, respectively)

3.5. A reporter system validated the functionality of *mefv*-targeting sgRNAs in 293T cells

Using the same logic behind GFP reporter assay, we tested the functionality of *mefv*-targeting sgRNAs (sgRNAs' table number). In this case, EFGP sequence was disrupted by a 100-bp intervening *mefv* fragment covering targeting sites of sgRNAs (G1-G4). Linear TGFP plasmid was used as a repair template to restore GFP in EGFP mutant 293T cells **(Figure 9A)**. In four mefv-targeting gRNAs, we observed an increase in GFP-positive cells percentage compared to untransfected control. sgRNA G2 gave rise to highest %GFP among the others**(Figure 9B)**.

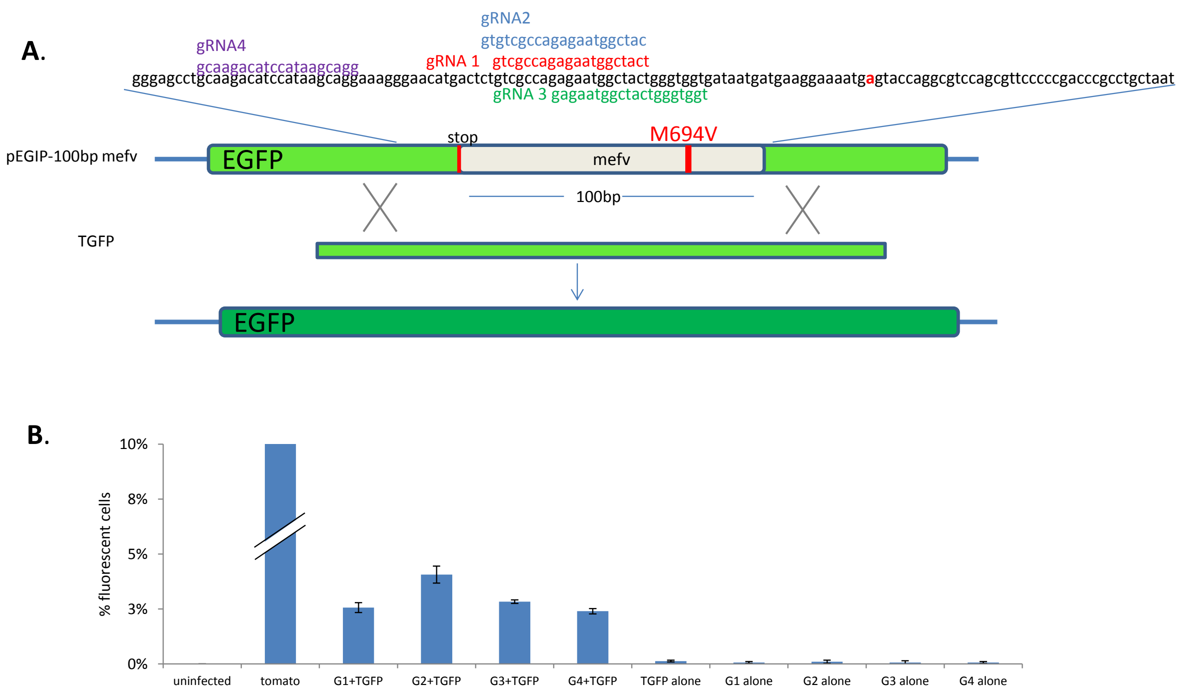

Figure 9. Generation of a reporter system to test the functionality of sgRNAs targeting *mefv* sequence.

(a) Schematic representation of pEGIP-100bp-mefv vector along with the locations of four *mefv*-targeting sgRNAs along the 100bp- sequence. Donor template TGFP (linear) was used to restore GFP expression in 293T cells transduced with pEGIP-100bp-mefv. (b) Percent GFP of pX459 (G1 to G4) transfected 293T cells by flow cytometry.

3.6. Linear donor template resulted in highest HR efficiency

Next, different repair templates were utilized to compare their efficiencies in terms of HR in EGFP mutant 293Ts. These include TGFP linear, circular and antisense GFP ssODN (Figure 8A). Flow data showed an increase in %GFP in all samples. We tried to find the most efficient *mefv*-targeting gRNA and donor template type in EGFP mutant 293T cells. According to the data, sgRNA2 and linear TGFP sample generated highest GFP expression with 3% GFP **(Figure 10B)**. Parallel to the finding, sgRNA2 was found to be the most efficient *mefv*-targeting sgRNA for all types of repair templates with 1.5%, 3.0% and 1.1% efficiencies.

A.

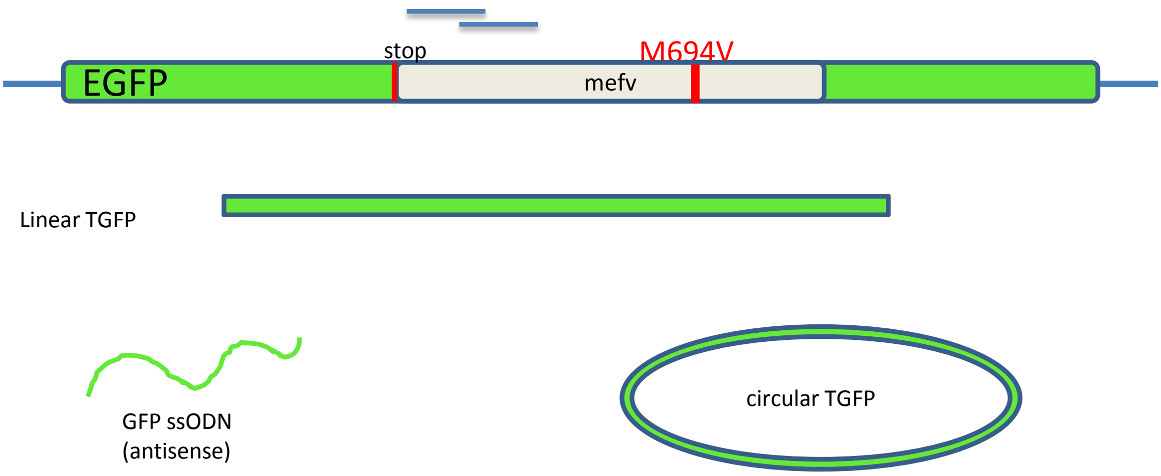

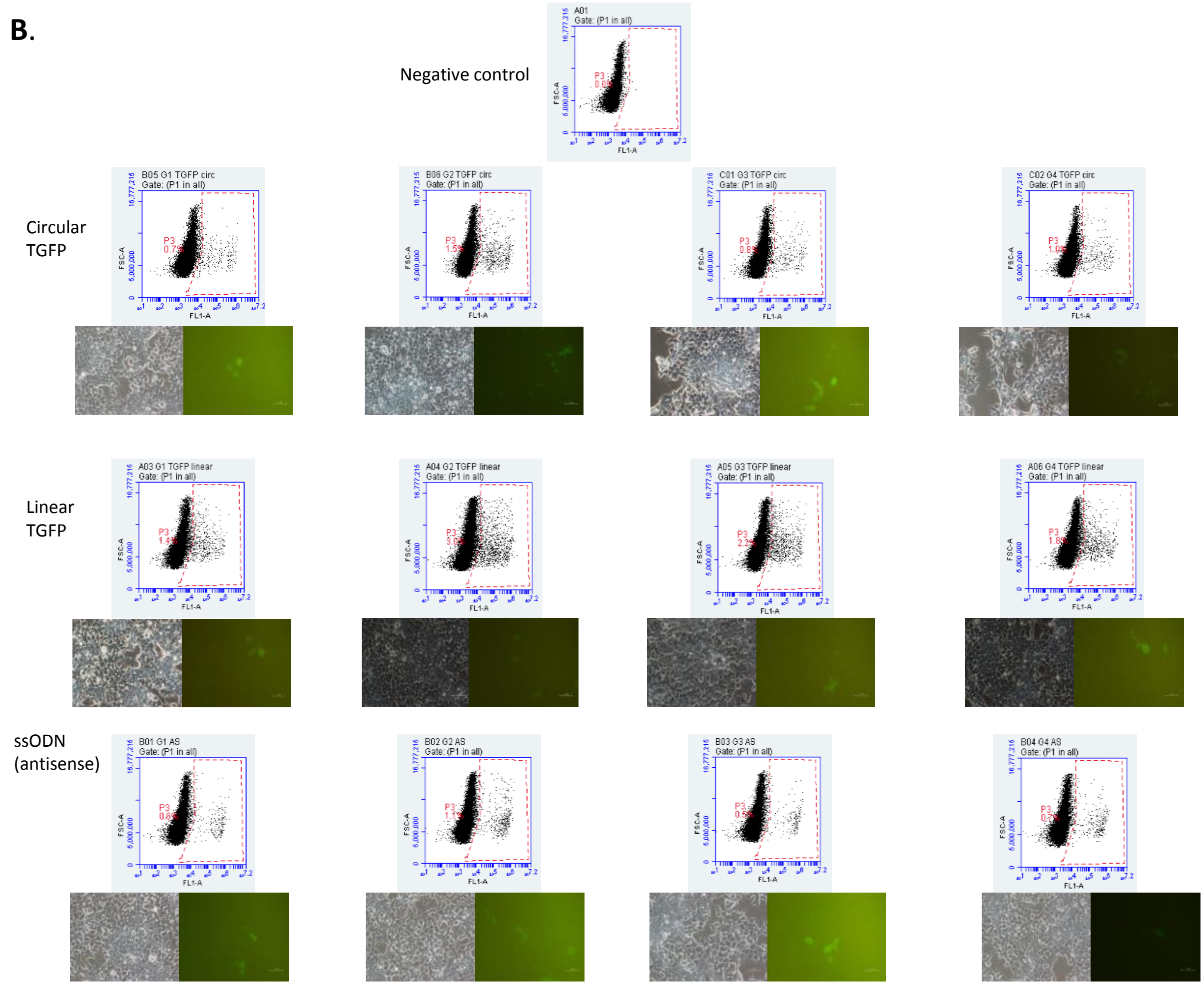

Cas9	-	+	+	+	+	+	+	+	+	+	+	+	+
gRNA1	-	+	-	-	-	+	-	-	-	+	-	-	-
gRNA2	-	-	+	-	-	-	+	-	-	-	+	-	-
gRNA3	-	-	-	+	-	-	-	+	-	-	-	+	-
gRNA4	-	-	-	-	+	-	-	-	+	-	-	-	+
TGFP linear	-	-	-	-	-	+	+	+	+	-	-	-	-
TGFP-circular	-	+	+	+	+	-	-	-	-	-	-	-	-
ssODN	-	-	-	-	-	-	-	-	-	+	+	+	+
%GFP positive	0.0	0.7	1.5	0.8	1.0	1.4	3.0	2.2	1.8	0.6	1.1	0.5	0.7

Figure 10. Testing different donor templates for HR efficiency.
(a) Linear and circular TGFP and antisense ssODN for GFP as donor templates along with pEGIP-100bp-mefv vector. (b) Percent GFP in different conditions by flow cytometry. Corresponding GFP-expressing cells were shown below.

3.7. *MEFV*-targeting sgRNAs generated DSB at endogenous *mefv* locus

In order to prove that *mefv*-targeting sgRNAs can act upon endogenous *mefv* sequence, we examined the presence indel mutations by NHEJ at that locus with the aid of T7 endonuclease assay. Upon transfection of sgRNAs and Cas9 into 293T cells and puromycin selection, DNA was collected at day 5 and T7 endonuclease assay showed expected bands in all samples. sgRNAs could target *mefv* locus and cause double-stranded cleavage **(Figure 11A,10B)**. Next, we wanted to monitor the activity of sgRNAs on a time-dependent manner and examined indel mutation rate by T7 endonuclease. This experiment indicated that double-stranded cleavage at the *mefv* locus was detectable at day 3 post-trasnfection of Crispr/Cas9 components and increased over time **(Figure 11C)**.

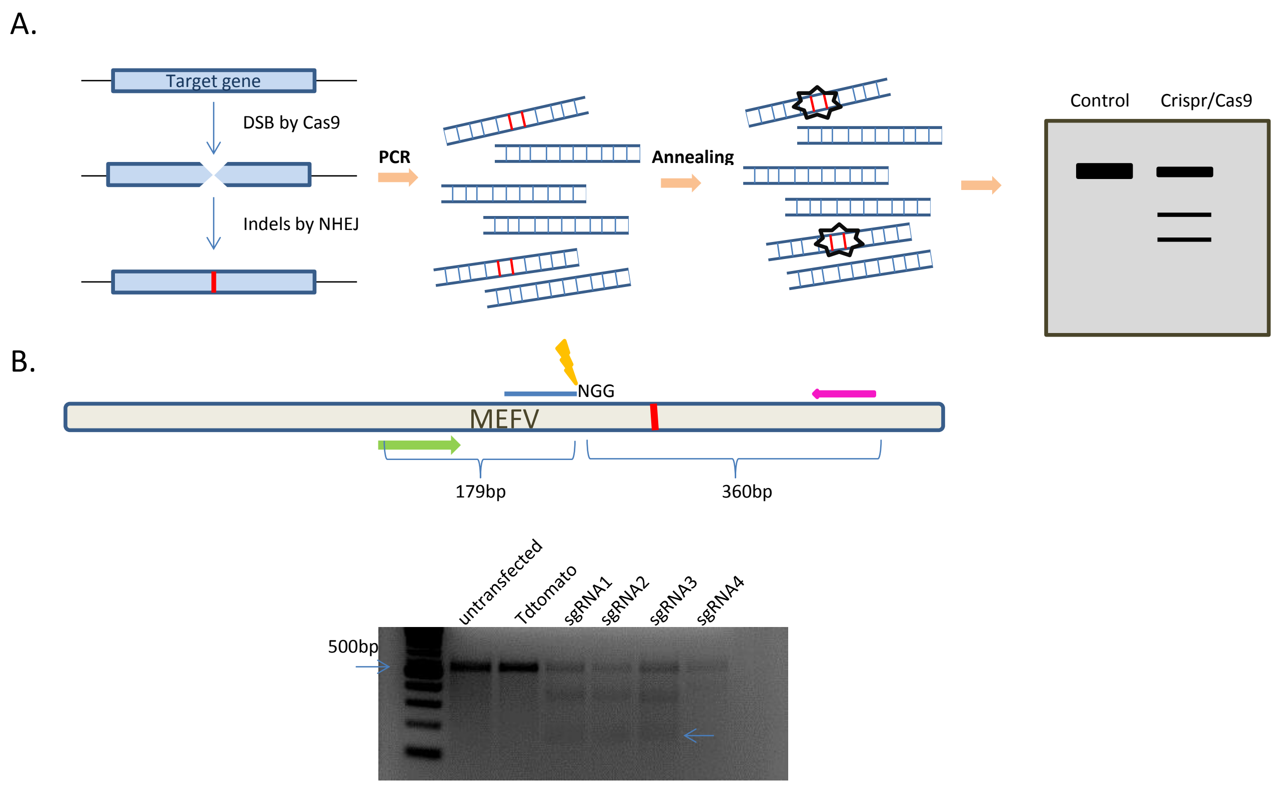

C.

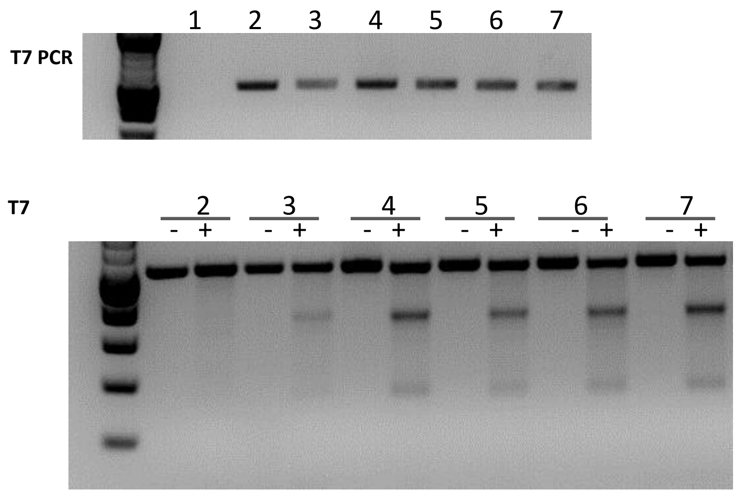

Figure 11. Confirmation of double-stranded cleavage by *MEFV*-targeting sgRNA2 at the endogenous *mefv* locus.
(a) Schematic representation of Surveyor and T7 Endonuclease assay. (b) Representation of Surveyor/T7 endonuclease primers. F- and R- primers were designed asymmetrically so as to obtain distinguishable fragments after endonuclease treatment. The expected bands were 179bp and 360bp for gRNA1& gRNA2, 185bp and 354bp for gRNA3, lastly 139bp and 400bp for gRNA4. (c) Kinetics of *mefv* cleavage in 293T cells. Top panel shows T7 PCR. Lower panel shows T7 endonuclease assay with/without T7 treatment. (1 - Untransfected, 2-Day2, 3-Day3, 4-Day4, 5-Day5, 6-Day6, 7-Day8)

3.8. Nucleofection of PBMC-iPSCs

We tested the efficiencies of iPSC nucleofection before transfecting Crispr/Cas9 components into patient iPSCs. For that, we used pmax-GFP plasmid supplied with different amounts under various conditions. GFP expression post-transfection of iPSCs were monitored by flow cytometry. As shown in figure 12, the highest %GFP was achieved on VTN plates in E8 medium (37.4%) but viability was too low (6.7%). Nucleofection on VTN plates in mTeSR1 medium resulted in low viability and low GFP expression.

We also investigated the effects of the presence of antibiotics in the transfection medium on nucleofection efficiency. Matrigel-coated plates in mTeSR1 medium without antibiotics resulted in higher GFP-positive cells than with antibiotics. Therefore, Matrigel-mTeSR1 without antibiotics was found to be the optimum in terms of cell viability and GFP expression. However, viability was also reduced as the amount of the vector used was increased **(Figure 12A, 12B)**.

A.

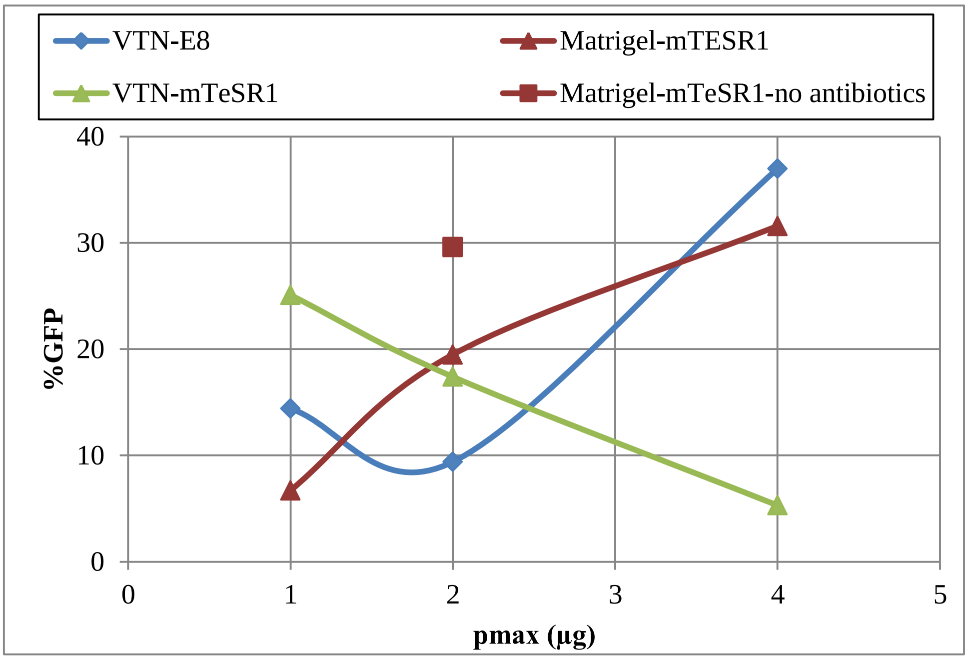

B.

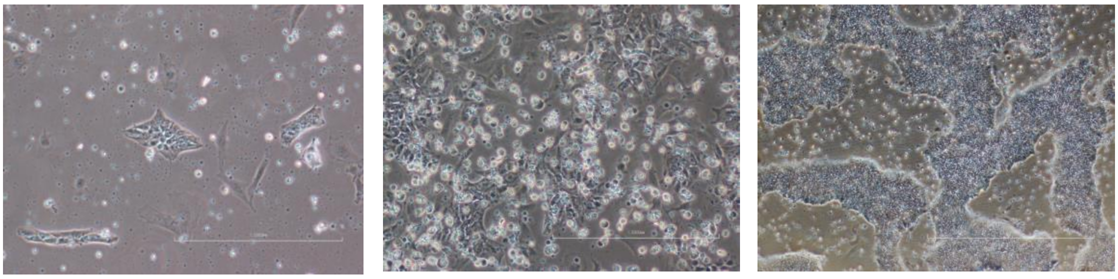

VTN- E8 (2 µg pmax)

Matrigel-mTeSR1 no pen/strep (2 µg pmax)

Matrigel-mTeSR1 with pen/strep (2 µg pmax)

Figure 12. Nucleofection of iPSC with different conditions.
(a) Graph of the amount of control plasmid vs %GFP. pmax-GFP vector was used in different amounts (1µg, 2 µg and 4 µg)as a nucleofection control. VTN-E8 indicates iPSCs on Vitronectin-coated plate with E8 medium. Matrigel-mTESR1 indicates the samples in Matrigel-coated plates in mTESR1 medium. Lastly, VTN-mTESR1 represents the samples on Vitronectin-coated plates in mTESR1 medium. Percent GFP was quantified by flow cytometry. (b) Images for different nucleofection conditions.

3.9. Cleavage of mefv locus in patient-iPSCs

We wanted to confirm if cleavage occurred at the *mefv* locus in patient-iPSCs subsequent to transient transfection of Cas9 and *mefv*-targeting gRNA G2. We also transduced patient-iPSCs in order them to continuously express Cas9 and gRNA G2 using lentiviral vectors. We monitored the cleavage by T7 endonuclease assay subsequent to puromycin selection. Transiently transfected cells did not exhibit any cleavage whereas the cells transduced with lentiCRISPR G2 slightly showed a pattern similar to that of 293Ts transfected with sgRNA2 (**Figure10B and Figure 13**). As a control, pEGIP transduced cells were used. However, the presence of non-specific DNA bands in all samples prevented us from arriving at a conclusive result.

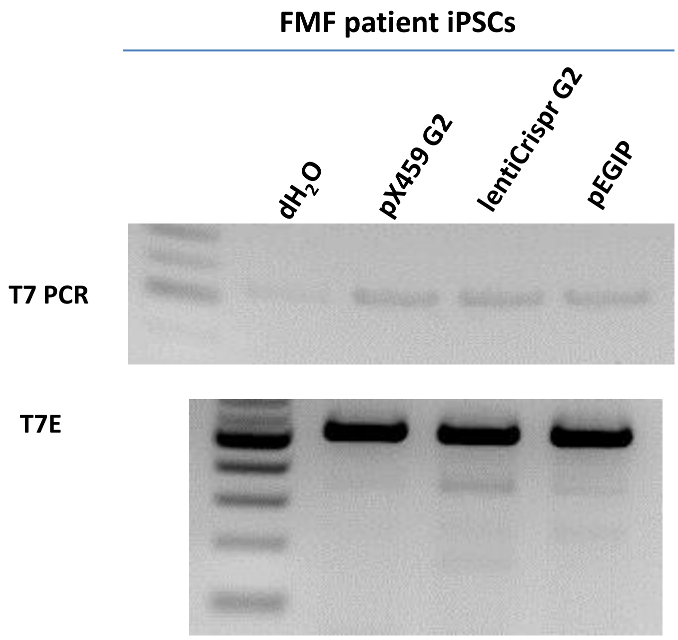

Figure 13. Double-stranded cleavage by G2 in patient iPSCs.
Upper lane shows T7 PCR. Lower lane indicates T7 Endonuclease assay after puromycin selection. The expected band for gRNA G2 is 179 and 360bp.

3.10. Detection of HR in FMF patient-derived iPSCs

In order to detect Crispr/Cas9-mediated homologous recombination in FMF patient-derived iPSCs, we utilized Amplification refractory mutation system (ARMS) PCR to amplify both wild-type and mutant alleles together with a control fragment within the same reaction tube. First, control experiment was designed with existing FMF patient and parent iPSC lines to confirm that we can observe wild type and mutant alleles. **Figure 14B** clearly demonstrates that FMF parent iPSCs are heterozygous, fibroblasts derived from H1 cell line (dH1f) and 293T cells are homozygous wild type and that FMF patient iPSCs are homozygous mutant for M694V. When the same experiment was repeated with FMF patient iPSCs transfected with Cas9 and gRNA2, we could not detect wild type allele. The rationale for the detection of Crispr-mediated HR was represented in **Figure 14A**.

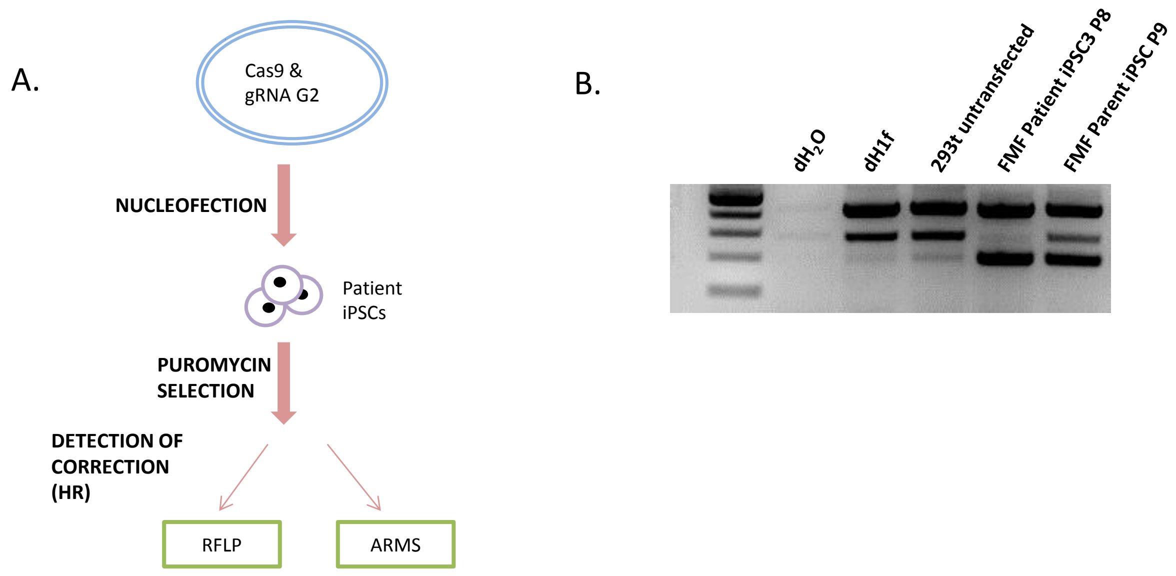

Figure 14. Diagram for the detection of HR in patient iPSCs.
(a) CRISPR-mediated HR can be detected either by RLFP or ARMS method subsequent to puromycin selection of transfected cells. (b) Control experiment with ARMS PCR demonstrating wild type and mutant alleles in various samples.

3.11. Design of *mefv* donor template

To be able to screen for corrected patient iPSCs, we designed a donor template where we could make use of restriction fragment length polymorphism (RFLP) by introducing *RsaI* restriction site in *mefv* donor template. Knowing that Cas9-sgRNA complex can re-cleave the repaired allele, we also created silent a mutation on sgRNA target site nearby PAM sequence to eliminate unwanted targeting. Upon recombination with this improved donor template, corrected patient iPSCs are expected to give a different pattern than that of parent, FMF patient and healthy control **(Figure 15).**

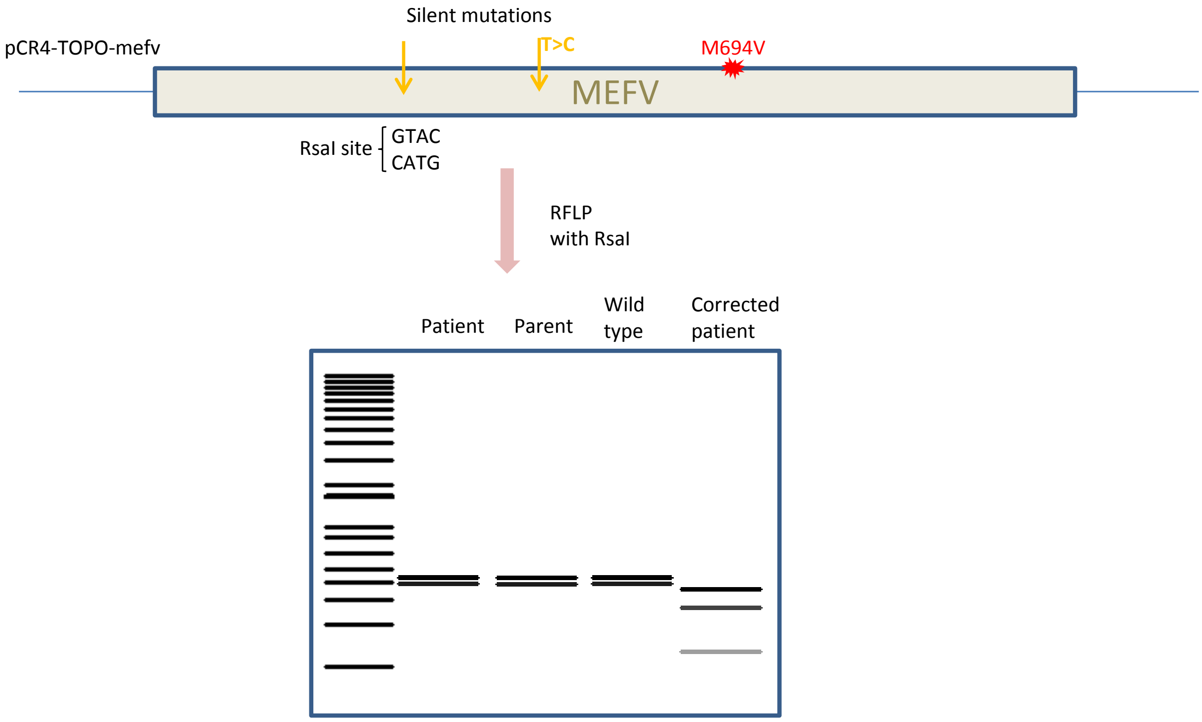

Figure 15. Design of a new *mefv* donor template.
The scheme of pCR4-TOPO-mefv vector is shown. The silent mutations around M694V mutation is shown with yellow arrows. One of the silent mutations generates a RsaI site in *mefv* sequence. Expected bands after RFLP were shown for all samples.

CHAPTER 4

DISCUSSION

4.1. Increasing the efficiency of homologous recombination

NHEJ-mediated repair of DSBs occurs in cells at any stage of the cell cycle, therfore gene knockout experiments via NHEJ-mediated insertion or deletion (indel) mutations has been showed to work efficiently[135]. However, homology-directed repair (HDR) which enables precise editing such as integration of a specific fragment or insertion of point mutations at the targeted site occurs only in dividing cells. Therefore, it has remained an inefficient process, creating a major challenge in precise gene editing [109]. In experiments presented in this thesis, GFP reporter assay in 293T cells with antisense and sense ssODNs yielded 0.5% and 0.3% HR rate, respectively (Figure 7B, 7C). Similarly, *MEFV*-targeting gRNAs in combination with different repair templates (tGFP linear/circular and ssODNs) revealed low HDR efficiency (0.5-3%) in 293T cells by flow cytometry (Figure 9B). HDR efficiency is expected to be even lower in patient-specific iPSCs. Recently, small compounds have been identified in order to elevate HDR rate [136]–[138]. Yu and his colleagues reported that L755507 increased HDR 3-fold for large fragment insertions and 9-fold for point mutation. It exhibited maximum effects at 5 μM within 24 hours post electroporation. It was also effective in a variety of cell types such as cancer cell lines, primary cells and neural stem cells. L755507 is a β3-adrenergic receptor partial agonist and it has been found that it increases lipolysis and metabolic rate in rhesus monkeys[134]. Alternatively, NHEJ inhibitors have been found to elevate HDR rates [136], [137]. These inhibitors involve compounds that target various proteins such as KU70, KU80 and DNA ligase IV [137]. Another study indicated that DNA ligase IV inhibitor Scr7 compound increased the efficiency of HDR in mammalian cells and in mice up to 19-fold[136]. When we performed the reporter assay of mefv-targeting gRNAs in patient iPSCs as we had done with 293Ts, CRISPR-mediated HDR efficiency with tGFP donor vector was 0.1% in patient-specific iPSCs compared to negative controls. Since it was not possible to conclude that CRISPR-mediated HDR occurred based on this data, it may be helpful to employ L755570 or Scr in order to obtain more reliable data in future experiments.

4.2. The specificity and off-target effects of Crispr/Cas9

One of the major concerns regarding CRISPR-mediated gene editing is potential off-target mutations. Undesired genetic modifications can be oncogenic and lead to proliferation of edited cells. In addition, they can disrupt the function of crucial genes. Each case would be harmful in terms of clinical applications. Off –target effects can occur at sites which bear high similarity to the on-target sites and has been reported be as high as 77% in terms of Crispr/Cas9 system [139]. The same study also argued that 7-12 bp seed sequence of gRNAs are sensitive to mismatches effecting Cas9 activity. In low similarity regions, nucleases have relatively low affinity due to mismatches between guide RNA and DNA. Nonetheless, nucleases may generate off-target mutations in those regions as well. Whole genome sequencing performed on transfected human iPSCs and human embryonic stem cells (HUES9) examined small indels, single nucleotide variants (SNVs), structural variants (SVs) such as chromosomal inversion, rearrangements and deletions and found no statistically significant off-target rate along the whole genome[140]. Mismatch sensitivity of Cas9 nuclease and low off-target mutation rate in hiPSCs have been confirmed by deep sequencing of predicted off-target sites and whole genome sequencing by other studies [141].

There are a number of approaches to minimize the frequency of off-target mutation. One of them is to improve targeting specificity of Cas9. Mutant Cas9 (D10A) generates a nick on a single strand. By using paired nickases and two separate gRNAs targeting opposite strands of the target site, it is possible to generate two nicks in close proximity, which are in turn processed as a double-stranded break within the cell. Because a single nick on the DNA can be repaired by base excision repair system [142], it drastically reduces possible off-target effect of Cas9 [143].

The other approach is the truncation of guide RNAs which reduces off-target effects by 5000-fold by shortening the complementarity between RNA and DNA[144]. The truncation may be generated by use of cDNA-derived sgRNA sequence or by adding two extra guanine nucleotides to 5’ end of gRNAs. Finally, inactive Cas9 (nickase) may be coupled with *FokI* increasing the specificity of Cas9[145]. One study has proved that Cas9 variants which have inactivating point mutations in the catalytic domains generated nicked open circular plasmids indicating that each domain is responsible for cleavage in one strand[108]. Inactive Cas9, Cas9D10A has been shown to yield HR rates comparable with active Cas9 but it resulted in lower NHEJ rate[105].

4.3. Increasing transfection efficiency of iPSCs

Transfection efficiency in human iPSCs have been reported as 60-70% [146]. We performed a set of nucleofection experiments according to the established protocols for human iPSC gene editing by using PGK-*Puro*-GFP plasmid as a transfection control, none which gave rise to GFP positive cells. In addition, the majority of the cells were killed subsequent to puromycin selection. This might have occurred from two reasons: Inefficient transfection or a SNP in pX459 plasmid reducing its efficacy. To eliminate the latter, we cloned our gRNAs into the more efficient pX459 Version 2. We next set up a control experiment by using pmax-GFP vector as a control which is much smaller than PGK-*Puro*-GFP. A variety of conditions were tested for nucleofection efficiency. We employed E8 and mTesR1 medium to distinguish their effects on transfection. The effect of antibiotic supplemented medium and the amount of the vector were the other factors that were tested. Finally we were able to obtain 35% efficiency with the cells on vitronectin coated plates in E8 medium (Figure 12). However, the viability of iPSCs was extremely low. We achieved comparable efficiencies with 2 µg pmax-GFP transfected iPSCs on Matrigel plates without penicillin/streptomycin and 4µg pmax-GFP transfected iPSCs on Matrigel-coated plates with mTeSR1 penicillin/streptomycin (29% and 31%). Comparing the viability of iPSCs, we decided on using 2 µg plasmid and medium without antibiotics. Low efficiency might also stem from relatively big sizes of control plasmids. When we used pEGIP plasmid as a transfection control, we were unable to obtain transfected cells.

To circumvent issues related to transfection, we tried infecting iPSCs with lentiCRISPR G2 and performed puromycin selection. Expanded cells were analyzed by T7 endonuclease assay and lentiCRISPR G2 infected iPSCs seemed to be mutated. pX459 transfected cells did not result in any mutant DNA band. Although this finding might be promising, it has to be repeated. Additionally, it is important to eliminate extra viral integrations on the genome to be able to obtain an isogenic control. Therefore, transfection conditions should be optimized rather than focusing on infections.

4.4. Investigating the role of pyrin in FMF in knockout cell lines

Pyrin plays role in inflammation and IL-1β secretion. Increased IL-1β production is one of the disease-related phenotypes in FMF patients. However, its exact role in IL-1β production is yet to be determined due to contradictory data in the literature. In order to further elucidate the role of pyrin in this mechanism, we aimed to knockout pyrin expression in THP-1 and HL-60 cells via Crispr/Cas9 gene editing system. We observed by T7 endonuclease assay that all of the three gRNAs designed for exon 1 of *mefv* were functional and generated indel mutations at the cleavage site (**Figure A1D** and **A1E**). Infected THP-1 cells were tested via ELISA and showed an increase in IL-1β production (data not shown). This finding supports the idea that pyrin inhibits IL-1β secretion. In order to generate pyrin knockout cell line, single cell clones of infected and positively selected cells were prepared to be checked with T7 endonuclease assay.

APPENDIX

The role of pyrin in inflammation has not yet known. In order to further understand the mechanism of FMF and to investigate the role of pyrin in IL-1β production, we aimed to generate a knockout cell line and check its phenotype to compare with the disease phenotype in terms of IL-1β production. To achieve this, we designed three sgRNAs targeting *mefv* exon1 and cloned them into lentiCRISPR vector. THP-1 and HL-60 cells were transduced. T7 endonuclease after selection showed that all of three sgRNAs caused indel mutation in exon1 **(Figure A1D and A1E)**.

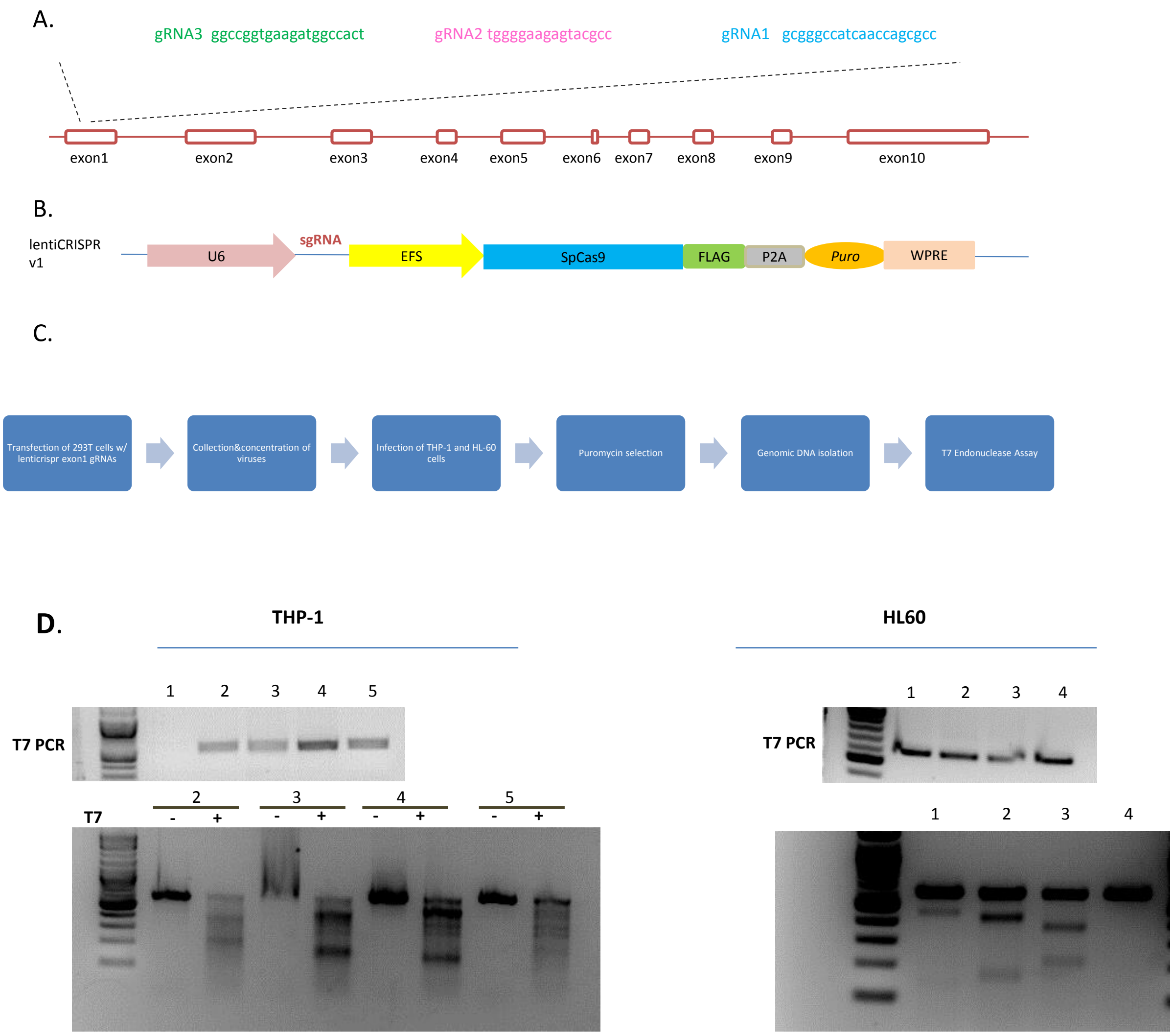

Figure A.1. Design and verification of gRNAs for *MEFV* knock-out cell lines.
(a) Three sgRNAs targeting exon1 of *mefv* locus are shown. (b) The representation of lentiCRISPR v1, cloning vector for exon1 gRNAs. (c) Flowchart for obtaining knock-out THP-1 cells. (d) T7 endonuclease assay for THP-1 and HL60 cells. Upper panel shows T7 PCR. Lower panel shows T7 digestion. Lane 1,2,3,4 and 5 correspond to exon1 gRNA1, gRNA2, gRNA3 and pEGIP infected samples for THP-1, respectively. Lanes 1,2,3 and 4 correspond to exon 1 gRNA3, gRNA2, gRNA1 and pEGIP, respectively.

BIBLIOGRAPHY

[1] K. Takahashi and S. Yamanaka, "Induction of pluripotent stem cells from mouse embryonic and adult fibroblast cultures by defined factors.," *Cell*, vol. 126, no. 4, pp. 663–76, Aug. 2006.

[2] K. Takahashi, K. Tanabe, M. Ohnuki, M. Narita, T. Ichisaka, K. Tomoda, and S. Yamanaka, "Induction of pluripotent stem cells from adult human fibroblasts by defined factors.," *Cell*, vol. 131, no. 5, pp. 861–72, Nov. 2007.

[3] Yu, Vodyanik, Smuga-Otto, Antosiewicz-Bourget, Frane, Tian, Nie, Jonsdottir, Ruotti, Stewart, Slukvin, and Thomson, "Induced Pluripotent Stem Cell Lines Derived from Human Somatic Cells," *Sci. (New York, NY)*, vol. 318, no. 5858, pp. 1917–20, 2007.

[4] A. Schnerch, C. Cerdan, and M. Bhatia, "Distinguishing between mouse and human pluripotent stem cell regulation: the best laid plans of mice and men.," *Stem Cells*, vol. 28, no. 3, pp. 419–30, Mar. 2010.

[5] K. Plath and W. E. Lowry, "Progress in understanding reprogramming to the induced pluripotent state," *Nat. Rev. Genet.*, vol. 12, no. 4, pp. 253–265, Apr. 2011.

[6] S. Eminli, A. Foudi, M. Stadtfeld, N. Maherali, T. Ahfeldt, G. Mostoslavsky, H. Hock, and K. Hochedlinger, "Differentiation stage determines potential of hematopoietic cells for reprogramming into induced pluripotent stem cells.," *Nat. Genet.*, vol. 41, no. 9, pp. 968–76, Sep. 2009.

[7] J. Yu, M. A. Vodyanik, K. Smuga-Otto, J. Antosiewicz-Bourget, J. L. Frane, S. Tian, J. Nie, G. A. Jonsdottir, V. Ruotti, R. Stewart, I. I. Slukvin, and J. A. Thomson, "Induced pluripotent stem cell lines derived from human somatic cells.," *Science*, vol. 318, no. 5858, pp. 1917–20, Dec. 2007.

[8] D. Hockemeyer, F. Soldner, E. G. Cook, Q. Gao, M. Mitalipova, and R. Jaenisch, "A drug-inducible system for direct reprogramming of human somatic cells to pluripotency.," *Cell Stem Cell*, vol. 3, no. 3, pp. 346–53, Sep. 2008.

[9] T. Aasen, A. Raya, M. J. Barrero, E. Garreta, A. Consiglio, F. Gonzalez, R. Vassena, J. Bilic, V. Pekarik, G. Tiscornia, M. Edel, S. Boue, and J. C. I. Belmonte, "Efficient and

rapid generation of induced pluripotent stem cells from human keratinocytes," *Nat Biotech*, vol. 26, no. 11, pp. 1276–1284, Nov. 2008.

[10] F. González, S. Boué, and J. C. I. Belmonte, "Methods for making induced pluripotent stem cells: reprogramming à la carte," *Nat. Rev. Genet.*, vol. 12, no. 4, pp. 231–242, 2011.

[11] J. Hanna, K. Saha, B. Pando, J. van Zon, C. J. Lengner, M. P. Creyghton, A. van Oudenaarden, and R. Jaenisch, "Direct cell reprogramming is a stochastic process amenable to acceleration," *Nature*, vol. 462, no. 7273, pp. 595–601, Dec. 2009.

[12] Y. Zhao, X. Yin, H. Qin, F. Zhu, H. Liu, W. Yang, Q. Zhang, C. Xiang, P. Hou, Z. Song, Y. Liu, J. Yong, P. Zhang, J. Cai, M. Liu, H. Li, Y. Li, X. Qu, K. Cui, W. Zhang, T. Xiang, Y. Wu, Y. Zhao, C. Liu, C. Yu, K. Yuan, J. Lou, M. Ding, and H. Deng, "Two Supporting Factors Greatly Improve the Efficiency of Human iPSC Generation," *Cell Stem Cell*, vol. 3, no. 5, pp. 475–479, Dec. 2015.

[13] N. Tsubooka, T. Ichisaka, K. Okita, K. Takahashi, M. Nakagawa, and S. Yamanaka, "Roles of Sall4 in the generation of pluripotent stem cells from blastocysts and fibroblasts," *Genes to Cells*, vol. 14, no. 6, pp. 683–694, 2009.

[14] I.-H. Park, R. Zhao, J. A. West, A. Yabuuchi, H. Huo, T. A. Ince, P. H. Lerou, M. W. Lensch, and G. Q. Daley, "Reprogramming of human somatic cells to pluripotency with defined factors.," *Nature*, vol. 451, no. 7175, pp. 141–6, Jan. 2008.

[15] J. Silva, O. Barrandon, J. Nichols, J. Kawaguchi, T. W. Theunissen, and A. Smith, "Promotion of reprogramming to ground state pluripotency by signal inhibition.," *PLoS Biol.*, vol. 6, no. 10, p. e253, Oct. 2008.

[16] R. L. Judson, J. E. Babiarz, M. Venere, and R. Blelloch, "Embryonic stem cell-specific microRNAs promote induced pluripotency.," *Nat. Biotechnol.*, vol. 27, no. 5, pp. 459–61, May 2009.

[17] D. Huangfu, R. Maehr, W. Guo, A. Eijkelenboom, M. Snitow, A. E. Chen, and D. A. Melton, "Induction of pluripotent stem cells by defined factors is greatly improved by small-molecule compounds.," *Nat. Biotechnol.*, vol. 26, no. 7, pp. 795–7, Jul. 2008.

[18] F. Xie, L. Ye, J. C. Chang, a. I. Beyer, J. Wang, M. O. Muench, and Y. W. Kan,

"Seamless gene correction of -thalassemia mutations in patient-specific iPSCs using CRISPR/Cas9 and piggyBac," *Genome Res.*, no. January 2016, p. gr.173427.114–, 2014.

[19] M. Stadtfeld, M. Nagaya, J. Utikal, G. Weir, and K. Hochedlinger, "Induced Pluripotent Stem Cells Generated Without Viral Integration," *Science (80-.).*, vol. 322, no. 5903, pp. 945–949, Nov. 2008.

[20] W. Zhou and C. R. Freed, "Adenoviral Gene Delivery Can Reprogram Human Fibroblasts to Induced Pluripotent Stem Cells," *Stem Cells*, vol. 27, no. 11, pp. 2667–2674, Nov. 2009.

[21] N. Fusaki, H. Ban, A. Nishiyama, K. Saeki, and M. Hasegawa, "Efficient induction of transgene-free human pluripotent stem cells using a vector based on Sendai virus, an RNA virus that does not integrate into the host genome.," *Proc. Jpn. Acad. Ser. B. Phys. Biol. Sci.*, vol. 85, no. 8, pp. 348–62, Jan. 2009.

[22] T. Seki, S. Yuasa, M. Oda, T. Egashira, K. Yae, D. Kusumoto, H. Nakata, S. Tohyama, H. Hashimoto, M. Kodaira, Y. Okada, H. Seimiya, N. Fusaki, M. Hasegawa, and K. Fukuda, "Generation of Induced Pluripotent Stem Cells from Human Terminally Differentiated Circulating T Cells," *Cell Stem Cell*, vol. 7, no. 1, pp. 11–14, Jul. 2010.

[23] K. Okita, H. Hong, K. Takahashi, and S. Yamanaka, "Generation of mouse-induced pluripotent stem cells with plasmid vectors.," *Nat. Protoc.*, vol. 5, no. 3, pp. 418–28, Mar. 2010.

[24] K. Okita, M. Nakagawa, H. Hyenjong, T. Ichisaka, and S. Yamanaka, "Generation of mouse induced pluripotent stem cells without viral vectors.," *Science*, vol. 322, no. 5903, pp. 949–53, Nov. 2008.

[25] J. Yu, K. Hu, K. Smuga-Otto, S. Tian, R. Stewart, I. I. Slukvin, and J. A. Thomson, "Human induced pluripotent stem cells free of vector and transgene sequences.," *Science*, vol. 324, no. 5928, pp. 797–801, May 2009.

[26] L. Warren, P. D. Manos, T. Ahfeldt, Y.-H. Loh, H. Li, F. Lau, W. Ebina, P. K. Mandal, Z. D. Smith, A. Meissner, G. Q. Daley, A. S. Brack, J. J. Collins, C. Cowan, T. M. Schlaeger, and D. J. Rossi, "Highly efficient reprogramming to pluripotency and directed differentiation of human cells with synthetic modified mRNA.," *Cell Stem*

Cell, vol. 7, no. 5, pp. 618–30, Nov. 2010.

[27] H. Zhou, S. Wu, J. Y. Joo, S. Zhu, D. W. Han, T. Lin, S. Trauger, G. Bien, S. Yao, Y. Zhu, G. Siuzdak, H. R. Schöler, L. Duan, and S. Ding, "Generation of induced pluripotent stem cells using recombinant proteins.," *Cell Stem Cell*, vol. 4, no. 5, pp. 381–4, May 2009.

[28] J. T. Dimos, K. T. Rodolfa, K. K. Niakan, L. M. Weisenthal, H. Mitsumoto, W. Chung, G. F. Croft, G. Saphier, R. Leibel, R. Goland, H. Wichterle, C. E. Henderson, and K. Eggan, "Induced pluripotent stem cells generated from patients with ALS can be differentiated into motor neurons.," *Science*, vol. 321, no. 5893, pp. 1218–21, Aug. 2008.

[29] I.-H. Park, N. Arora, H. Huo, N. Maherali, T. Ahfeldt, A. Shimamura, M. W. Lensch, C. Cowan, K. Hochedlinger, and G. Q. Daley, "Disease-specific induced pluripotent stem cells.," *Cell*, vol. 134, no. 5, pp. 877–86, Sep. 2008.

[30] H. Inoue, N. Nagata, H. Kurokawa, and S. Yamanaka, "iPS cells: a game changer for future medicine.," *EMBO J.*, vol. 33, no. 5, pp. 409–17, Mar. 2014.

[31] T. Tanaka, K. Takahashi, M. Yamane, S. Tomida, S. Nakamura, K. Oshima, A. Niwa, R. Nishikomori, N. Kambe, H. Hara, M. Mitsuyama, N. Morone, J. E. Heuser, T. Yamamoto, A. Watanabe, A. Sato-Otsubo, S. Ogawa, I. Asaka, T. Heike, S. Yamanaka, T. Nakahata, and M. K. Saito, "Induced pluripotent stem cells from CINCA syndrome patients as a model for dissecting somatic mosaicism and drug discovery," *Blood*, vol. 120, no. 6, pp. 1299–1308, Jun. 2012.

[32] A. D. Ebert, J. Yu, F. F. Rose, V. B. Mattis, C. L. Lorson, J. A. Thomson, and C. N. Svendsen, "Induced pluripotent stem cells from a spinal muscular atrophy patient.," *Nature*, vol. 457, no. 7227, pp. 277–80, Jan. 2009.

[33] M. C. N. Marchetto, C. Carromeu, A. Acab, D. Yu, G. W. Yeo, Y. Mu, G. Chen, F. H. Gage, and A. R. Muotri, "A model for neural development and treatment of Rett syndrome using human induced pluripotent stem cells.," *Cell*, vol. 143, no. 4, pp. 527–39, Nov. 2010.

[34] K. J. Brennand, A. Simone, J. Jou, C. Gelboin-Burkhart, N. Tran, S. Sangar, Y. Li, Y. Mu, G. Chen, D. Yu, S. McCarthy, J. Sebat, and F. H. Gage, "Modelling schizophrenia

using human induced pluripotent stem cells," *Nature*, vol. 473, no. 7346, pp. 221–225, Apr. 2011.

[35] F. Soldner, D. Hockemeyer, C. Beard, Q. Gao, G. W. Bell, E. G. Cook, G. Hargus, A. Blak, O. Cooper, M. Mitalipova, O. Isacson, and R. Jaenisch, "Parkinson's disease patient-derived induced pluripotent stem cells free of viral reprogramming factors.," *Cell*, vol. 136, no. 5, pp. 964–77, Mar. 2009.

[36] T. T. Onder and G. Q. Daley, "New lessons learned from disease modeling with induced pluripotent stem cells," *Curr. Opin. Genet. Dev.*, vol. 22, no. 5, pp. 500–508, Oct. 2012.

[37] K. Musunuru, "Genome editing of human pluripotent stem cells to generate human cellular disease models.," *Dis. Model. Mech.*, vol. 6, no. 4, pp. 896–904, Jul. 2013.

[38] K. Martins-Taylor, B. S. Nisler, S. M. Taapken, T. Compton, L. Crandall, K. D. Montgomery, M. Lalande, and R.-H. Xu, "Recurrent copy number variations in human induced pluripotent stem cells," *Nat. Biotechnol.*, vol. 29, no. 6, pp. 488–491, Jun. 2011.

[39] S. M. Taapken, B. S. Nisler, M. A. Newton, T. L. Sampsell-Barron, K. A. Leonhard, E. M. McIntire, and K. D. Montgomery, "Karotypic abnormalities in human induced pluripotent stem cells and embryonic stem cells," *Nat. Biotechnol.*, vol. 29, no. 4, pp. 313–314, Apr. 2011.

[40] J. Sandoe and K. Eggan, "Opportunities and challenges of pluripotent stem cell neurodegenerative disease models.," *Nat. Neurosci.*, vol. 16, no. 7, pp. 780–9, Jul. 2013.

[41] Q. Ding, Y.-K. Lee, E. A. K. Schaefer, D. T. Peters, A. Veres, K. Kim, N. Kuperwasser, D. L. Motola, T. B. Meissner, W. T. Hendriks, M. Trevisan, R. M. Gupta, A. Moisan, E. Banks, M. Friesen, R. T. Schinzel, F. Xia, A. Tang, Y. Xia, E. Figueroa, A. Wann, T. Ahfeldt, L. Daheron, F. Zhang, L. L. Rubin, L. F. Peng, R. T. Chung, K. Musunuru, and C. A. Cowan, "A TALEN genome-editing system for generating human stem cell-based disease models.," *Cell Stem Cell*, vol. 12, no. 2, pp. 238–51, Feb. 2013.

[42] F. P. Di Giorgio, M. A. Carrasco, M. C. Siao, T. Maniatis, and K. Eggan, "Non-cell

autonomous effect of glia on motor neurons in an embryonic stem cell-based ALS model.," *Nat. Neurosci.*, vol. 10, no. 5, pp. 608–14, May 2007.

[43] J. A. Doudna and E. Charpentier, "The new frontier of genome engineering with CRISPR-Cas9," *Science (80-.).*, vol. 346, no. 6213, pp. 1258096–1258096, Nov. 2014.

[44] Z. Sandor and A. Bredberg, "Deficient DNA repair of triple helix-directed double psoralen damage in human cells," *FEBS Lett.*, vol. 374, no. 2, pp. 287–291, Oct. 1995.

[45] S. A. Strobel and P. B. Dervan, "Single-site enzymatic cleavage of yeast genomic DNA mediated by triple helix formation," *Nature*, vol. 350, no. 6314, pp. 172–174, Mar. 1991.

[46] J. Yang, S. Zimmerly, P. S. Perlman, and A. M. Lambowitz, "Efficient integration of an intron RNA into double-stranded DNA by reverse splicing.," *Nature*, vol. 381, no. 6580, pp. 332–5, May 1996.

[47] B. S. Chevalier, T. Kortemme, M. S. Chadsey, D. Baker, R. J. Monnat, and B. L. Stoddard, "Design, Activity, and Structure of a Highly Specific Artificial Endonuclease," *Mol. Cell*, vol. 10, no. 4, pp. 895–905, Oct. 2002.

[48] A. L. Firth, T. Menon, G. S. Parker, S. J. Qualls, B. M. Lewis, E. Ke, C. T. Dargitz, R. Wright, A. Khanna, F. H. Gage, and I. M. Verma, "Functional Gene Correction for Cystic Fibrosis in Lung Epithelial Cells Generated from Patient iPSCs.," *Cell Rep.*, vol. 12, no. 9, pp. 1385–90, Aug. 2015.

[49] A. M. Crane, P. Kramer, J. H. Bui, W. J. Chung, X. S. Li, M. L. Gonzalez-Garay, F. Hawkins, W. Liao, D. Mora, S. Choi, J. Wang, H. C. Sun, D. E. Paschon, D. Y. Guschin, P. D. Gregory, D. N. Kotton, M. C. Holmes, E. J. Sorscher, and B. R. Davis, "Targeted Correction and Restored Function of the CFTR Gene in Cystic Fibrosis Induced Pluripotent Stem Cells.," *Stem cell reports*, vol. 4, no. 4, pp. 569–77, Apr. 2015.

[50] P. Xu, Y. Tong, X. Liu, T. Wang, L. Cheng, B. Wang, X. Lv, Y. Huang, and D. Liu, "Both TALENs and CRISPR/Cas9 directly target the HBB IVS2-654 (C > T) mutation in β-thalassemia-derived iPSCs.," *Sci. Rep.*, vol. 5, p. 12065, Jan. 2015.

[51] X. Huang, Y. Wang, W. Yan, C. Smith, Z. Ye, J. Wang, Y. Gao, L. Mendelsohn, and

L. Cheng, “Production of Gene-Corrected Adult Beta Globin Protein in Human Erythrocytes Differentiated from Patient iPSCs After Genome Editing of the Sickle Point Mutation.,” *Stem Cells*, vol. 33, no. 5, pp. 1470–9, May 2015.

[52] B. Song, Y. Fan, W. He, D. Zhu, X. Niu, D. Wang, Z. Ou, M. Luo, and X. Sun, “Improved Hematopoietic Differentiation Efficiency of Gene-Corrected Beta-Thalassemia Induced Pluripotent Stem Cells by CRISPR/Cas9 System,” *Stem Cells Dev.*, vol. 24, no. 9, pp. 1053–1065, 2015.

[53] V. Sebastiano, M. L. Maeder, J. F. Angstman, B. Haddad, C. Khayter, D. T. Yeo, M. J. Goodwin, J. S. Hawkins, C. L. Ramirez, L. F. Z. Batista, S. E. Artandi, M. Wernig, and J. K. Joung, “In situ genetic correction of the sickle cell anemia mutation in human induced pluripotent stem cells using engineered zinc finger nucleases.,” *Stem Cells*, vol. 29, no. 11, pp. 1717–26, Nov. 2011.

[54] N. Holt, J. Wang, K. Kim, G. Friedman, X. Wang, V. Taupin, G. M. Crooks, D. B. Kohn, P. D. Gregory, M. C. Holmes, and P. M. Cannon, “Human hematopoietic stem/progenitor cells modified by zinc-finger nucleases targeted to CCR5 control HIV-1 in vivo.,” *Nat. Biotechnol.*, vol. 28, no. 8, pp. 839–47, Aug. 2010.

[55] L. Ye, J. Wang, A. I. Beyer, F. Teque, T. J. Cradick, Z. Qi, J. C. Chang, G. Bao, M. O. Muench, J. Yu, J. A. Levy, and Y. W. Kan, “Seamless modification of wild-type induced pluripotent stem cells to the natural CCR5 32 mutation confers resistance to HIV infection,” *Proc. Natl. Acad. Sci.*, vol. 111, no. 26, pp. 9591–9596, Jun. 2014.

[56] C. Smith, L. Abalde-Atristain, C. He, B. R. Brodsky, E. M. Braunstein, P. Chaudhari, Y.-Y. Jang, L. Cheng, and Z. Ye, “Efficient and allele-specific genome editing of disease loci in human iPSCs.,” *Mol. Ther.*, vol. 23, no. 3, pp. 570–7, Mar. 2015.

[57] J. P. Connelly, E. M. Kwon, Y. Gao, N. S. Trivedi, A. G. Elkahloun, M. S. Horwitz, L. Cheng, and P. P. Liu, “Targeted correction of RUNX1 mutation in FPD patient-specific induced pluripotent stem cells rescues megakaryopoietic defects,” *Blood*, vol. 124, no. 12, pp. 1926–1930, Aug. 2014.

[58] H. Iizuka, Y. Kagoya, K. Kataoka, A. Yoshimi, M. Miyauchi, K. Taoka, K. Kumano, T. Yamamoto, A. Hotta, S. Arai, and M. Kurokawa, “Targeted gene correction of RUNX1 in induced pluripotent stem cells derived from familial platelet disorder with

propensity to myeloid malignancy restores normal megakaryopoiesis," *Exp. Hematol.*, vol. 43, no. 10, pp. 849–857, Oct. 2015.

[59] A.-K. Dreyer, D. Hoffmann, N. Lachmann, M. Ackermann, D. Steinemann, B. Timm, U. Siler, J. Reichenbach, M. Grez, T. Moritz, A. Schambach, and T. Cathomen, "TALEN-mediated functional correction of X-linked chronic granulomatous disease in patient-derived induced pluripotent stem cells.," *Biomaterials*, vol. 69, pp. 191–200, Nov. 2015.

[60] R. K. Merling, C. L. Sweeney, J. Chu, A. Bodansky, U. Choi, D. L. Priel, D. B. Kuhns, H. Wang, S. Vasilevsky, S. S. De Ravin, T. Winkler, C. E. Dunbar, J. Zou, K. A. Zarember, J. I. Gallin, S. M. Holland, and H. L. Malech, "An AAVS1-Targeted Minigene Platform for Correction of iPSCs From All Five Types of Chronic Granulomatous Disease," *Mol. Ther.*, vol. 23, no. 1, pp. 147–157, Oct. 2014.

[61] H. L. Li, N. Fujimoto, N. Sasakawa, S. Shirai, T. Ohkame, T. Sakuma, M. Tanaka, N. Amano, A. Watanabe, H. Sakurai, T. Yamamoto, S. Yamanaka, and A. Hotta, "Precise correction of the dystrophin gene in duchenne muscular dystrophy patient induced pluripotent stem cells by TALEN and CRISPR-Cas9.," *Stem cell reports*, vol. 4, no. 1, pp. 143–54, Jan. 2015.

[62] S. Raitano, L. Ordovàs, L. De Muynck, W. Guo, I. Espuny-Camacho, M. Geraerts, S. Khurana, K. Vanuytsel, B. I. Tóth, T. Voets, R. Vandenberghe, T. Cathomen, L. Van Den Bosch, P. Vanderhaeghen, P. Van Damme, and C. M. Verfaillie, "Restoration of progranulin expression rescues cortical neuron generation in an induced pluripotent stem cell model of frontotemporal dementia.," *Stem cell reports*, vol. 4, no. 1, pp. 16–24, Jan. 2015.

[63] I. Karakikes, F. Stillitano, M. Nonnenmacher, C. Tzimas, D. Sanoudou, V. Termglinchan, C.-W. Kong, S. Rushing, J. Hansen, D. Ceholski, F. Kolokathis, D. Kremastinos, A. Katoulis, L. Ren, N. Cohen, J. M. I. H. Gho, D. Tsiapras, A. Vink, J. C. Wu, F. W. Asselbergs, R. A. Li, J.-S. Hulot, E. G. Kranias, and R. J. Hajjar, "Correction of human phospholamban R14del mutation associated with cardiomyopathy using targeted nucleases and combination therapy.," *Nat. Commun.*, vol. 6, p. 6955, Jan. 2015.

[64] S. H. Rahman, J. Kuehle, C. Reimann, T. Mlambo, J. Alzubi, M. L. Maeder, H. Riedel,

P. Fisch, T. Cantz, C. Rudolph, C. Mussolino, J. K. Joung, A. Schambach, and T. Cathomen, “Rescue of DNA-PK Signaling and T-Cell Differentiation by Targeted Genome Editing in a prkdc Deficient iPSC Disease Model.,” *PLoS Genet.*, vol. 11, no. 5, p. e1005239, May 2015.

[65] G.-H. Liu, K. Suzuki, M. Li, J. Qu, N. Montserrat, C. Tarantino, Y. Gu, F. Yi, X. Xu, W. Zhang, S. Ruiz, N. Plongthongkum, K. Zhang, S. Masuda, E. Nivet, Y. Tsunekawa, R. D. Soligalla, A. Goebl, E. Aizawa, N. Y. Kim, J. Kim, I. Dubova, Y. Li, R. Ren, C. Benner, A. del Sol, J. Bueren, J. P. Trujillo, J. Surralles, E. Cappelli, C. Dufour, C. R. Esteban, and J. C. Izpisua Belmonte, “Modelling Fanconi anemia pathogenesis and therapeutics using integration-free patient-derived iPSCs.,” *Nat. Commun.*, vol. 5, p. 4330, Jan. 2014.

[66] S. M. Choi, Y. Kim, J. S. Shim, J. T. Park, R.-H. Wang, S. D. Leach, J. O. Liu, C. Deng, Z. Ye, and Y.-Y. Jang, “Efficient drug screening and gene correction for treating liver disease using patient-specific stem cells.,” *Hepatology*, vol. 57, no. 6, pp. 2458–68, Jun. 2013.

[67] C.-Y. Park, J. Kim, J. Kweon, J. S. Son, J. S. Lee, J.-E. Yoo, S.-R. Cho, J.-H. Kim, J.-S. Kim, and D.-W. Kim, “Targeted inversion and reversion of the blood coagulation factor 8 gene in human iPS cells using TALENs,” *Proc. Natl. Acad. Sci.*, vol. 111, no. 25, pp. 9253–9258, Jun. 2014.

[68] P. Reinhardt, B. Schmid, L. F. Burbulla, D. C. Schöndorf, L. Wagner, M. Glatza, S. Höing, G. Hargus, S. A. Heck, A. Dhingra, G. Wu, S. Müller, K. Brockmann, T. Kluba, M. Maisel, R. Krüger, D. Berg, Y. Tsytsyura, C. S. Thiel, O.-E. Psathaki, J. Klingauf, T. Kuhlmann, M. Klewin, H. Müller, T. Gasser, H. R. Schöler, and J. Sterneckert, “Genetic correction of a LRRK2 mutation in human iPSCs links parkinsonian neurodegeneration to ERK-dependent changes in gene expression.,” *Cell Stem Cell*, vol. 12, no. 3, pp. 354–67, Mar. 2013.

[69] H. Fong, C. Wang, J. Knoferle, D. Walker, M. E. Balestra, L. M. Tong, L. Leung, K. L. Ring, W. W. Seeley, A. Karydas, M. A. Kshirsagar, A. L. Boxer, K. S. Kosik, B. L. Miller, and Y. Huang, “Genetic correction of tauopathy phenotypes in neurons derived from human induced pluripotent stem cells.,” *Stem cell reports*, vol. 1, no. 3, pp. 226–34, Jan. 2013.

[70] M. C. An, N. Zhang, G. Scott, D. Montoro, T. Wittkop, S. Mooney, S. Melov, and L. M. Ellerby, “Genetic correction of Huntington’s disease phenotypes in induced pluripotent stem cells.,” *Cell Stem Cell*, vol. 11, no. 2, pp. 253–63, Aug. 2012.

[71] F. D. Urnov, E. J. Rebar, M. C. Holmes, H. S. Zhang, and P. D. Gregory, “Genome editing with engineered zinc finger nucleases.,” *Nat. Rev. Genet.*, vol. 11, no. 9, pp. 636–46, Sep. 2010.

[72] M. Bibikova, K. Beumer, J. K. Trautman, and D. Carroll, “Enhancing gene targeting with designed zinc finger nucleases.,” *Science*, vol. 300, no. 5620, p. 764, May 2003.

[73] M. Bibikova, M. Golic, K. G. Golic, and D. Carroll, “Targeted chromosomal cleavage and mutagenesis in Drosophila using zinc-finger nucleases.,” *Genetics*, vol. 161, no. 3, pp. 1169–75, Jul. 2002.

[74] J. Miller, A. D. McLachlan, and A. Klug, “Repetitive zinc-binding domains in the protein transcription factor IIIA from Xenopus oocytes.,” *EMBO J.*, vol. 4, no. 6, pp. 1609–14, Jun. 1985.

[75] E. S. Vanamee, S. Santagata, and A. K. Aggarwal, “FokI requires two specific DNA sites for cleavage.,” *J. Mol. Biol.*, vol. 309, no. 1, pp. 69–78, May 2001.

[76] K. J. Beumer, J. K. Trautman, A. Bozas, J.-L. Liu, J. Rutter, J. G. Gall, and D. Carroll, “Efficient gene targeting in Drosophila by direct embryo injection with zinc-finger nucleases.,” *Proc. Natl. Acad. Sci. U. S. A.*, vol. 105, no. 50, pp. 19821–6, Dec. 2008.

[77] J. E. Foley, J.-R. J. Yeh, M. L. Maeder, D. Reyon, J. D. Sander, R. T. Peterson, and J. K. Joung, “Rapid Mutation of Endogenous Zebrafish Genes Using Zinc Finger Nucleases Made by Oligomerized Pool ENgineering (OPEN),” *PLoS One*, vol. 4, no. 2, p. e4348, Feb. 2009.

[78] T. Mashimo, A. Takizawa, B. Voigt, K. Yoshimi, H. Hiai, T. Kuramoto, and T. Serikawa, “Generation of Knockout Rats with X-Linked Severe Combined Immunodeficiency (X-SCID) Using Zinc-Finger Nucleases,” *PLoS One*, vol. 5, no. 1, p. e8870, Jan. 2010.

[79] Y. Santiago, E. Chan, P.-Q. Liu, S. Orlando, L. Zhang, F. D. Urnov, M. C. Holmes, D. Guschin, A. Waite, J. C. Miller, E. J. Rebar, P. D. Gregory, A. Klug, and T. N.

Collingwood, “Targeted gene knockout in mammalian cells by using engineered zinc-finger nucleases.,” *Proc. Natl. Acad. Sci. U. S. A.*, vol. 105, no. 15, pp. 5809–14, Apr. 2008.

[80] F. D. Urnov, J. C. Miller, Y.-L. Lee, C. M. Beausejour, J. M. Rock, S. Augustus, A. C. Jamieson, M. H. Porteus, P. D. Gregory, and M. C. Holmes, “Highly efficient endogenous human gene correction using designed zinc-finger nucleases.,” *Nature*, vol. 435, no. 7042, pp. 646–51, Jun. 2005.

[81] A. Lombardo, P. Genovese, C. M. Beausejour, S. Colleoni, Y.-L. Lee, K. A. Kim, D. Ando, F. D. Urnov, C. Galli, P. D. Gregory, M. C. Holmes, and L. Naldini, “Gene editing in human stem cells using zinc finger nucleases and integrase-defective lentiviral vector delivery.,” *Nat. Biotechnol.*, vol. 25, no. 11, pp. 1298–306, Nov. 2007.

[82] B. F. Benabdallah, E. Allard, S. Yao, G. Friedman, P. D. Gregory, N. Eliopoulos, J. Fradette, J. L. Spees, E. Haddad, M. C. Holmes, and C. M. Beauséjour, “Targeted gene addition to human mesenchymal stromal cells as a cell-based plasma-soluble protein delivery platform.,” *Cytotherapy*, vol. 12, no. 3, pp. 394–9, May 2010.

[83] A. J. Bogdanove and D. F. Voytas, “TAL effectors: customizable proteins for DNA targeting.,” *Science*, vol. 333, no. 6051, pp. 1843–6, Sep. 2011.

[84] S. Kay, S. Hahn, E. Marois, G. Hause, and U. Bonas, “A bacterial effector acts as a plant transcription factor and induces a cell size regulator.,” *Science*, vol. 318, no. 5850, pp. 648–51, Oct. 2007.

[85] M. J. Moscou and A. J. Bogdanove, “A simple cipher governs DNA recognition by TAL effectors.,” *Science*, vol. 326, no. 5959, p. 1501, Dec. 2009.

[86] M. Christian, T. Cermak, E. L. Doyle, C. Schmidt, F. Zhang, A. Hummel, A. J. Bogdanove, and D. F. Voytas, “Targeting DNA double-strand breaks with TAL effector nucleases.,” *Genetics*, vol. 186, no. 2, pp. 757–61, Oct. 2010.

[87] Q. Ding, Y.-K. Lee, E. A. K. Schaefer, D. T. Peters, A. Veres, K. Kim, N. Kuperwasser, D. L. Motola, T. B. Meissner, W. T. Hendriks, M. Trevisan, R. M. Gupta, A. Moisan, E. Banks, M. Friesen, R. T. Schinzel, F. Xia, A. Tang, Y. Xia, E. Figueroa, A. Wann, T. Ahfeldt, L. Daheron, F. Zhang, L. L. Rubin, L. F. Peng, R. T. Chung, K. Musunuru, and C. A. Cowan, “A TALEN genome-editing system for

generating human stem cell-based disease models.," *Cell Stem Cell*, vol. 12, no. 2, pp. 238–51, Feb. 2013.

[88] J. C. Miller, S. Tan, G. Qiao, K. A. Barlow, J. Wang, D. F. Xia, X. Meng, D. E. Paschon, E. Leung, S. J. Hinkley, G. P. Dulay, K. L. Hua, I. Ankoudinova, G. J. Cost, F. D. Urnov, H. S. Zhang, M. C. Holmes, L. Zhang, P. D. Gregory, and E. J. Rebar, "A TALE nuclease architecture for efficient genome editing.," *Nat. Biotechnol.*, vol. 29, no. 2, pp. 143–8, Feb. 2011.

[89] C. Mussolino, R. Morbitzer, F. Lütge, N. Dannemann, T. Lahaye, and T. Cathomen, "A novel TALE nuclease scaffold enables high genome editing activity in combination with low toxicity.," *Nucleic Acids Res.*, vol. 39, no. 21, pp. 9283–93, Nov. 2011.

[90] C. Smith, A. Gore, W. Yan, L. Abalde-Atristain, Z. Li, C. He, Y. Wang, R. A. Brodsky, K. Zhang, L. Cheng, and Z. Ye, "Whole-Genome Sequencing Analysis Reveals High Specificity of CRISPR/Cas9 and TALEN-Based Genome Editing in Human iPSCs," *Cell Stem Cell*, vol. 15, no. 1, pp. 12–13, Jul. 2014.

[91] K. Suzuki, C. Yu, J. Qu, M. Li, X. Yao, T. Yuan, A. Goebl, S. Tang, R. Ren, E. Aizawa, F. Zhang, X. Xu, R. D. Soligalla, F. Chen, J. Kim, N. Y. Kim, H.-K. Liao, C. Benner, C. R. Esteban, Y. Jin, G.-H. Liu, Y. Li, and J. C. Izpisua Belmonte, "Targeted gene correction minimally impacts whole-genome mutational load in human-disease-specific induced pluripotent stem cell clones.," *Cell Stem Cell*, vol. 15, no. 1, pp. 31–6, Jul. 2014.

[92] M. Holkers, I. Maggio, J. Liu, J. M. Janssen, F. Miselli, C. Mussolino, A. Recchia, T. Cathomen, and M. A. F. V Gonçalves, "Differential integrity of TALE nuclease genes following adenoviral and lentiviral vector gene transfer into human cells.," *Nucleic Acids Res.*, vol. 41, no. 5, p. e63, Mar. 2013.

[93] L. Yang, M. Guell, S. Byrne, J. L. Yang, A. De Los Angeles, P. Mali, J. Aach, C. Kim-Kiselak, A. W. Briggs, X. Rios, P.-Y. Huang, G. Daley, and G. Church, "Optimization of scarless human stem cell genome editing.," *Nucleic Acids Res.*, vol. 41, no. 19, pp. 9049–61, Oct. 2013.

[94] D. Bhaya, M. Davison, and R. Barrangou, "CRISPR-Cas systems in bacteria and archaea: versatile small RNAs for adaptive defense and regulation.," *Annu. Rev.*

Genet., vol. 45, pp. 273–97, Jan. 2011.

[95] P. Horvath and R. Barrangou, “CRISPR/Cas, the immune system of bacteria and archaea.,” *Science*, vol. 327, no. 5962, pp. 167–70, Jan. 2010.

[96] H. Deveau, J. E. Garneau, and S. Moineau, “CRISPR/Cas system and its role in phage-bacteria interactions.,” *Annu. Rev. Microbiol.*, vol. 64, pp. 475–93, Jan. 2010.

[97] R. Jansen, J. D. A. van Embden, W. Gaastra, and L. M. Schouls, “Identification of genes that are associated with DNA repeats in prokaryotes,” *Mol. Microbiol.*, vol. 43, no. 6, pp. 1565–1575, Mar. 2002.

[98] Y. Ishino, H. Shinagawa, K. Makino, M. Amemura, and A. Nakata, “Nucleotide sequence of the iap gene, responsible for alkaline phosphatase isozyme conversion in Escherichia coli, and identification of the gene product.,” *J. Bacteriol.*, vol. 169, no. 12, pp. 5429–33, Dec. 1987.

[99] F. J. M. Mojica, C. Diez-Villasenor, E. Soria, and G. Juez, “Biological significance of a family of regularly spaced repeats in the genomes of Archaea, Bacteria and mitochondria,” *Mol. Microbiol.*, vol. 36, no. 1, pp. 244–246, Apr. 2000.

[100] A. Bolotin, B. Quinquis, A. Sorokin, and S. D. Ehrlich, “Clustered regularly interspaced short palindrome repeats (CRISPRs) have spacers of extrachromosomal origin.,” *Microbiology*, vol. 151, no. Pt 8, pp. 2551–61, Aug. 2005.

[101] F. J. M. Mojica, C. Díez-Villaseñor, J. García-Martínez, and E. Soria, “Intervening sequences of regularly spaced prokaryotic repeats derive from foreign genetic elements.,” *J. Mol. Evol.*, vol. 60, no. 2, pp. 174–82, Feb. 2005.

[102] R. Barrangou, C. Fremaux, H. Deveau, M. Richards, P. Boyaval, S. Moineau, D. A. Romero, and P. Horvath, “CRISPR provides acquired resistance against viruses in prokaryotes.,” *Science*, vol. 315, no. 5819, pp. 1709–12, Mar. 2007.

[103] S. J. J. Brouns, M. M. Jore, M. Lundgren, E. R. Westra, R. J. H. Slijkhuis, A. P. L. Snijders, M. J. Dickman, K. S. Makarova, E. V Koonin, and J. van der Oost, “Small CRISPR RNAs guide antiviral defense in prokaryotes.,” *Science*, vol. 321, no. 5891, pp. 960–4, Aug. 2008.

[104] L. A. Marraffini and E. J. Sontheimer, “CRISPR interference limits horizontal gene

transfer in staphylococci by targeting DNA.," *Science*, vol. 322, no. 5909, pp. 1843–5, Dec. 2008.

[105] P. D. Hsu, E. S. Lander, and F. Zhang, "Development and Applications of CRISPR-Cas9 for Genome Engineering.," *Cell*, vol. 157, no. 6, pp. 1262–1278, Jun. 2014.

[106] E. Deltcheva, K. Chylinski, C. M. Sharma, K. Gonzales, Y. Chao, Z. A. Pirzada, M. R. Eckert, J. Vogel, and E. Charpentier, "CRISPR RNA maturation by trans-encoded small RNA and host factor RNase III.," *Nature*, vol. 471, no. 7340, pp. 602–7, Mar. 2011.

[107] M. Jinek, F. Jiang, D. W. Taylor, S. H. Sternberg, E. Kaya, E. Ma, C. Anders, M. Hauer, K. Zhou, S. Lin, M. Kaplan, A. T. Iavarone, E. Charpentier, E. Nogales, and J. A. Doudna, "Structures of Cas9 endonucleases reveal RNA-mediated conformational activation.," *Science*, vol. 343, no. 6176, p. 1247997, Mar. 2014.

[108] H. Nishimasu, F. A. Ran, P. D. Hsu, S. Konermann, S. I. Shehata, N. Dohmae, R. Ishitani, F. Zhang, and O. Nureki, "Crystal structure of Cas9 in complex with guide RNA and target DNA.," *Cell*, vol. 156, no. 5, pp. 935–49, Feb. 2014.

[109] P. Mali, L. Yang, K. M. Esvelt, J. Aach, M. Guell, J. E. DiCarlo, J. E. Norville, and G. M. Church, "RNA-guided human genome engineering via Cas9.," *Science*, vol. 339, no. 6121, pp. 823–6, Feb. 2013.

[110] P. D. Hsu, E. S. Lander, and F. Zhang, "Development and Applications of CRISPR-Cas9 for Genome Engineering.," *Cell*, vol. 157, no. 6, pp. 1262–1278, Jun. 2014.

[111] Y. Zhang, N. Heidrich, B. J. Ampattu, C. W. Gunderson, H. S. Seifert, C. Schoen, J. Vogel, and E. J. Sontheimer, "Processing-Independent CRISPR RNAs Limit Natural Transformation in Neisseria meningitidis," *Mol. Cell*, vol. 50, no. 4, pp. 488–503, May 2013.

[112] M. Jinek, K. Chylinski, I. Fonfara, M. Hauer, J. A. Doudna, and E. Charpentier, "A programmable dual-RNA-guided DNA endonuclease in adaptive bacterial immunity.," *Science*, vol. 337, no. 6096, pp. 816–21, Aug. 2012.

[113] M. Jinek, A. East, A. Cheng, S. Lin, E. Ma, and J. Doudna, "RNA-programmed genome editing in human cells.," *Elife*, vol. 2, p. e00471, Jan. 2013.

[114] L. Cong, F. A. Ran, D. Cox, S. Lin, R. Barretto, N. Habib, P. D. Hsu, X. Wu, W. Jiang, L. A. Marraffini, and F. Zhang, "Multiplex genome engineering using CRISPR/Cas systems.," *Science*, vol. 339, no. 6121, pp. 819–23, Feb. 2013.

[115] M. R. Lieber, "The mechanism of double-strand DNA break repair by the nonhomologous DNA end-joining pathway.," *Annu. Rev. Biochem.*, vol. 79, pp. 181–211, Jan. 2010.

[116] Y.-F. Chang, J. S. Imam, and M. F. Wilkinson, "The nonsense-mediated decay RNA surveillance pathway.," *Annu. Rev. Biochem.*, vol. 76, pp. 51–74, Jan. 2007.

[117] F. Chen, S. M. Pruett-Miller, Y. Huang, M. Gjoka, K. Duda, J. Taunton, T. N. Collingwood, M. Frodin, and G. D. Davis, "High-frequency genome editing using ssDNA oligonucleotides with zinc-finger nucleases.," *Nat. Methods*, vol. 8, no. 9, pp. 753–5, Sep. 2011.

[118] P. Rouet, F. Smih, and M. Jasin, "Expression of a site-specific endonuclease stimulates homologous recombination in mammalian cells.," *Proc. Natl. Acad. Sci. U. S. A.*, vol. 91, no. 13, pp. 6064–8, Jun. 1994.

[119] B.-K. Chou, P. Mali, X. Huang, Z. Ye, S. N. Dowey, L. M. Resar, C. Zou, Y. A. Zhang, J. Tong, and L. Cheng, "Efficient human iPS cell derivation by a non-integrating plasmid from blood cells with unique epigenetic and gene expression signatures.," *Cell Res.*, vol. 21, no. 3, pp. 518–29, Mar. 2011.

[120] N. Ma, B. Liao, H. Zhang, L. Wang, Y. Shan, Y. Xue, K. Huang, S. Chen, X. Zhou, Y. Chen, D. Pei, and G. Pan, "Transcription activator-like effector nuclease (TALEN)-mediated gene correction in integration-free β-thalassemia induced pluripotent stem cells.," *J. Biol. Chem.*, vol. 288, no. 48, pp. 34671–9, Nov. 2013.

[121] F. Onen, "Familial Mediterranean fever," *Rheumatol. Int.*, vol. 26, no. 6, pp. 489–496, Nov. 2005.

[122] M. Lidar and a. Livneh, "Familial mediterranean fever: Clinical, molecular and management advancements," *Neth. J. Med.*, vol. 65, no. 9, pp. 318–324, 2007.

[123] E. Ben-Chetrit and I. Touitou, "Familial Mediterranean Fever in the World," *Arthritis Rheum.*, vol. 61, no. 10, pp. 1447–1453, Oct. 2009.

[124] I. Sari, M. Birlik, and T. Kasifoglu, “Familial Mediterranean fever: An updated review,” *Eur. J. Rheumatol.*, vol. 1, no. 1, pp. 21–33, Mar. 2014.

[125] M. Tunca, S. Akar, F. Onen, H. Ozdogan, O. Kasapcopur, F. Yalcinkaya, E. Tutar, S. Ozen, R. Topaloglu, E. Yilmaz, M. Arici, A. Bakkaloglu, N. Besbas, T. Akpolat, A. Dinc, and E. Erken, “Familial Mediterranean fever (FMF) in Turkey: results of a nationwide multicenter study.,” *Medicine (Baltimore).*, vol. 84, no. 1, pp. 1–11, Jan. 2005.

[126] F. Albayrak, N. Y. Selcuk, A. R. Odabas, R. Cetinkaya, and I. Pirim, “Genotype-phenotype correlation in patients with familial Mediterranean fever in East Anatolia (Turkey).,” *Genet. Test. Mol. Biomarkers*, vol. 14, no. 3, pp. 325–8, Jun. 2010.

[127] M. Centola, G. Wood, D. M. Frucht, J. Galon, M. Aringer, C. Farrell, D. W. Kingma, M. E. Horwitz, E. Mansfield, S. M. Holland, J. J. O’Shea, H. F. Rosenberg, H. L. Malech, and D. L. Kastner, “The gene for familial Mediterranean fever, MEFV, is expressed in early leukocyte development and is regulated in response to inflammatory mediators.,” *Blood*, vol. 95, no. 10, pp. 3223–3231, 2000.

[128] S. Grandemange, I. Aksentijevich, I. Jeru, A. Gul, and I. Touitou, “The regulation of MEFV expression and its role in health and familial Mediterranean fever.,” *Genes Immun.*, vol. 12, no. 7, pp. 497–503, 2011.

[129] C. Stehlik, L. Fiorentino, A. Dorfleutner, J.-M. Bruey, E. M. Ariza, J. Sagara, and J. C. Reed, “The PAAD/PYRIN-family protein ASC is a dual regulator of a conserved step in nuclear factor kappaB activation pathways.,” *J. Exp. Med.*, vol. 196, no. 12, pp. 1605–15, Dec. 2002.

[130] J. J. Chae, G. Wood, S. L. Masters, K. Richard, G. Park, B. J. Smith, and D. L. Kastner, “The B30.2 domain of pyrin, the familial Mediterranean fever protein, interacts directly with caspase-1 to modulate IL-1beta production,” *Proc. Natl. Acad. Sci.*, vol. 103, no. 26, pp. 9982–9987, Jun. 2006.

[131] P. R. Hesker, M. Nguyen, M. Kovarova, J. P.-Y. Ting, and B. H. Koller, “Genetic loss of murine pyrin, the Familial Mediterranean Fever protein, increases interleukin-1β levels.,” *PLoS One*, vol. 7, no. 11, p. e51105, 2012.

[132] “Advances in the understanding of familial Mediterranean fever and possibilities for

targeted therapy. - Google’da Ara.” [Online]. Available: https://www.google.com.tr/search?q=Advances+in+the+understanding+of+familial+Mediterranean+fever+and+possibilities+for+targeted+therapy.&oq=Advances+in+the+understanding+of+familial+Mediterranean+fever+and+possibilities+for+targeted+therapy.&aqs=chrome..69i57.460j0j7&sourceid=chrome&es_sm=93&ie=UTF-8. [Accessed: 09-Jan-2016].

[133] K. Fidan, G. Kavaklıoğlu, A. Ebrahimi, C. Özlü, N. Z. Ay, A. Ruacan, A. Gül, and T. T. Önder, “Generation of integration-free induced pluripotent stem cells from a patient with Familial Mediterranean Fever (FMF),” *Stem Cell Res.*, vol. 15, no. 3, pp. 694–696, 2015.

[134] P. D. Hsu, D. A. Scott, J. A. Weinstein, F. A. Ran, S. Konermann, V. Agarwala, Y. Li, E. J. Fine, X. Wu, O. Shalem, T. J. Cradick, L. A. Marraffini, G. Bao, and F. Zhang, “DNA targeting specificity of RNA-guided Cas9 nucleases.,” *Nat. Biotechnol.*, vol. 31, no. 9, pp. 827–32, Sep. 2013.

[135] T. Wang, J. J. Wei, D. M. Sabatini, and E. S. Lander, “Genetic screens in human cells using the CRISPR-Cas9 system.,” *Science*, vol. 343, no. 6166, pp. 80–4, Jan. 2014.

[136] W. Fernandes, K. Smart, Y. Smith, H. Phipps, A. Panoutsou, K. B. Krause, R. Hughes, and P. Campbell, “Genome editing,” *Nature*, vol. 528, no. 7581, pp. S1–S17, 2015.

[137] V. T. Chu, T. Weber, B. Wefers, W. Wurst, S. Sander, K. Rajewsky, and R. Kühn, “Increasing the efficiency of homology-directed repair for CRISPR-Cas9-induced precise gene editing in mammalian cells.,” *Nat. Biotechnol.*, vol. 33, no. 5, pp. 543–548, 2015.

[138] P. S. Cells, C. Yu, Y. Liu, S. Ding, L. S. Qi, C. Yu, Y. Liu, T. Ma, K. Liu, S. Xu, Y. Zhang, H. Liu, M. La Russa, and M. Xie, “Small Molecules Enhance CRISPR Genome Editing in Small Molecules Enhance CRISPR Genome Editing in Pluripotent Stem Cells,” *Cell Stem Cell*, vol. 16, no. 2, pp. 142–147, 2015.

[139] V. Pattanayak, S. Lin, J. P. Guilinger, E. Ma, J. A. Doudna, and D. R. Liu, “High-throughput profiling of off-target DNA cleavage reveals RNA-programmed Cas9 nuclease specificity.,” *Nat. Biotechnol.*, vol. 31, no. 9, pp. 839–43, Sep. 2013.

[140] A. Veres, B. S. Gosis, Q. Ding, R. Collins, A. Ragavendran, H. Brand, S. Erdin, C. A.

Cowan, M. E. Talkowski, and K. Musunuru, "Low incidence of off-target mutations in individual CRISPR-Cas9 and TALEN targeted human stem cell clones detected by whole-genome sequencing.," *Cell Stem Cell*, vol. 15, no. 1, pp. 27–30, Jul. 2014.

[141] L. Yang, D. Grishin, G. Wang, J. Aach, C.-Z. Zhang, R. Chari, J. Homsy, X. Cai, Y. Zhao, J.-B. Fan, C. Seidman, J. Seidman, W. Pu, and G. Church, "Targeted and genome-wide sequencing reveal single nucleotide variations impacting specificity of Cas9 in human stem cells.," *Nat. Commun.*, vol. 5, p. 5507, Jan. 2014.

[142] K. W. Caldecott, "Single-strand break repair and genetic disease.," *Nat. Rev. Genet.*, vol. 9, no. 8, pp. 619–31, Aug. 2008.

[143] S. W. Cho, S. Kim, Y. Kim, J. Kweon, H. S. Kim, S. Bae, and J.-S. Kim, "Analysis of off-target effects of CRISPR/Cas-derived RNA-guided endonucleases and nickases.," *Genome Res.*, vol. 24, no. 1, pp. 132–41, Jan. 2014.

[144] Y. Fu, J. D. Sander, D. Reyon, V. M. Cascio, and J. K. Joung, "Improving CRISPR-Cas nuclease specificity using truncated guide RNAs.," *Nat. Biotechnol.*, vol. 32, no. 3, pp. 279–84, Mar. 2014.

[145] J. P. Guilinger, D. B. Thompson, and D. R. Liu, "Fusion of catalytically inactive Cas9 to FokI nuclease improves the specificity of genome modification.," *Nat. Biotechnol.*, vol. 32, no. 6, pp. 577–82, Jun. 2014.

[146] S. M. Byrne, P. Mali, and G. M. Church, "Genome editing in human stem cells.," *Methods Enzymol.*, vol. 546, pp. 119–38, Jan. 2014.